



HAL
open science

Material approaches to active tissue mechanics

Wang Xi, Thuan Beng Saw, Delphine Delacour, Chwee Teck Lim, Benoit
Ladoux

► **To cite this version:**

Wang Xi, Thuan Beng Saw, Delphine Delacour, Chwee Teck Lim, Benoit Ladoux. Material approaches to active tissue mechanics. *Nature Reviews Materials*, 2019, 4 (1), pp.23-44. 10.1038/s41578-018-0066-z . hal-03453579

HAL Id: hal-03453579

<https://hal.science/hal-03453579>

Submitted on 27 Oct 2023

HAL is a multi-disciplinary open access archive for the deposit and dissemination of scientific research documents, whether they are published or not. The documents may come from teaching and research institutions in France or abroad, or from public or private research centers.

L'archive ouverte pluridisciplinaire **HAL**, est destinée au dépôt et à la diffusion de documents scientifiques de niveau recherche, publiés ou non, émanant des établissements d'enseignement et de recherche français ou étrangers, des laboratoires publics ou privés.

Material approaches to active tissue mechanics

Wang Xi^{1*}, Thuan Beng Saw^{2,3*}, Delphine Delacour¹, Chwee Teck Lim^{2,3}, Benoit Ladoux^{1,3}

¹Institut Jacques Monod (IJM), CNRS UMR 7592 & Université Paris Diderot, Paris, France

²Department of Biomedical Engineering, National University of Singapore, Singapore 117576

³Mechanobiology Institute (MBI), National University of Singapore, Singapore 117411

Correspondence to W. X.: wang.xi@ijm.fr; C.T.L.: ctlim@nus.edu.sg; B.L. benoit.ladoux@ijm.fr

* These authors contributed equally to this work.

Abstract

Communities of epithelial cells demonstrate close intercellular communications and highly ordered coordination in their motility. In the cohort, each cells are constitutive energy-consuming agents and they generate forces and interact with others via cell-cell junctions. The force rebalancing within the population that can be invoked by various external stimuli and endogenous cellular events then leads to self-adjustment of tissue internal contractile stresses and organization, concomitant with distinct overall dynamics. To unveil the mechanisms of various tissue dynamics, it is required to understand how epithelia decode environmental inputs into mechanical principles that underpinned many vital biological processes, including homeostasis, morphogenesis, and metastasis. Thus, significant interdisciplinary efforts have recently been made towards coupling cellular milieus with the latest advent of materials science and microengineering techniques to create controllable arenas for epithelial studies. By modulating the mechanical contacts at cell/material interfaces, researchers can study aspects of *in vivo* epithelial dynamics and how tissues regulate mechanosensing mechanisms. In this review, we summarize the state-of-the-art material methodologies to mimic *in vivo* conditions and study epithelial mechanics. Especially, we discuss tissues as active materials and try to understand tissue rheological properties and active behaviors at different length scales. We further focus on the interdisciplinary study of the active, emergent mechanical properties of tissue and its complex interface with the microenvironment.

Introduction

Epithelia are one of the four basic kinds of animal tissue and is central to the construction of the body, representing more than 60% of the vertebrate body's cells¹. *In vivo*, these tissues play crucial roles in many biological processes, including wound healing², embryonic development³, morphogenesis⁴, homeostasis⁴ and metastasis⁵. During these processes, epithelia demonstrate fascinating physical properties as they can flow like a fluid^{6,7} or behave as a solid⁶, and exhibit various complicated behaviours, such as collective migration⁸, oscillation^{9,10}, turbulent motion¹¹, active cell rearrangements¹², cell division and extrusion^{13,14}. These phenomena take place in various circumstances containing different biochemical and biophysical cues, and the epithelium needs to interpret the microenvironment cues to commit to distinct strategies.

Apart from genes and biochemical signaling cascades, mechanical factors of the tissue and its microenvironment are now known to have an equivalent potency in influencing epithelial behaviours⁸. Cells

sense the mechanical environment by exerting forces to the substrate largely through actomyosin-dependent contraction, mediated by the active walking of myosin motor proteins along actin filaments. These forces can also propagate through the tissue *via* cell-cell junctions notably through E-cadherin-mediated adherens junctions (AJs) that stitch cells together¹⁵. Cell-substrate and cell-cell junctions are under constant mechanical stress¹⁶, which can activate the remodeling of these sites¹⁷ and further trigger cell signaling events within the tissue⁸. Hence, from cytoskeleton networks to large cell assemblies, a certain rheological behaviour of biological materials is a complicated compromise among competing forces, cellular events, and exogenous stimuli. For instance, the motor protein activity influences the viscoelasticity of cytoskeleton and the network can be significantly stiffened in a stress-dependent fashion¹⁸. The actin cytoskeleton within single cells can respond to substrate stiffness changes by remodeling and rheological adaptation¹⁹. At tissue level, epithelia sense their mechanical environment with cell-substrate adhesive complex and show durotaxis in response to rigid changes *in vivo* during the neural crest migration in the *Xenopus laevis*²⁰ as well as *in vitro* on a surface of stiffness gradient²¹. To counterbalance endogenic strain, tissue can trigger live cell delamination at sites of highest crowding and buffer epithelial hyperplasia, such as during homeostasis in the *Drosophila* germ band¹⁴, zebrafish fins¹³, and colon epithelia¹³. On the other hand, the reciprocal mechanical effects between epithelia and their microenvironment is commonly seen. As an illustrative example, during *Drosophila* oogenesis, disorganized extracellular matrix (ECM) can be remodeled into global polarized, restrictive ECM with uniform actin bundle alignment through coordinated rotation of follicular epithelial cells^{3,22}. Other than these, the interaction between tissues and their microenvironment is also implicated in numerous pathological processes, such as cancer metastasis. *In vivo*, the tumor mass is confined by a collagen-rich microenvironment²³, where the basement membrane and stroma presents a significant physical barrier for the escape of cancer cells²⁴. The structural aspects of the ECM have been found to provide mechanosensing cues for cancer metastasis, as ECM fibril alignment²⁵ and specific fibril orientation²⁶ were crucial determinants of cell invasion. On the other, invasive cancer cells can remodel the stroma to promote the invasion. In *in vitro* hydrogel system, it was found that cancer-associated fibroblasts (CAFs) can produce fibronectin and align them by producing elevated actomyosin-mediated traction forces, and integrin-based adhesion allowed efficient cancer cell migration on these aligned fibers²⁷. In short, living systems from molecular to multicellular assemblies are active materials that interact, probe and respond to their microenvironment.

Further, the epithelia couples with the microenvironment in complex ways. Studies using *in vivo* models to decipher such relationships are limited as many important biophysical aspects in the microenvironment are typically intertwined²⁸, including material stiffness, spatial confinement, porosity, viscoelasticity, material degradability, and binding affinity. Further, tissue mechanical forces *in vivo* have been highly difficult if not impossible to measure directly. To overcome these challenges, collaborative efforts by biologists, physicists, engineers and materials scientists have replicated and studied many biological phenomena *in vitro* using cell biology, microengineering, materials, and modeling approaches. Indeed, collective cell migration under confinement, collective durotaxis²¹, geometrical and stretching-controlled epithelial extrusion^{13,29}, and epithelial growth regulation in two dimension (2D)³⁰ and 3D³¹ have been investigated. These achievements have allowed a deeper understanding of tissues as active matters³² and the way they interact with the material⁸. *In vitro* studies have helped to dissect the effects of multiple mechanical cues of the microenvironment on cellular behavior, and in turn, the in-depth insights of tissue mechanics have promoted the development of new materials and designer methods for bioengineering, *in vitro* modelling, immunotherapy, and gene therapy. Here we review the recent achievements from the viewpoint of materials science in addressing different questions about tissue mechanical properties and behavior.

Engineered tissue/material interface

The development of microengineered biomimetic materials for epithelial studies has seen a trend moving from 2D to 3D³³ and from materials of static properties to those of dynamic nature³⁴. The application of various microfabrication techniques has helped to shed light on the mechanotransduction mechanisms of multicellular assemblies when encountering the complex external cues, such as spatial distribution of adhesive biomolecules, rigidity, topography, geometry, and mechanical stress. In this section, we summarize the technologies for microengineering the epithelial microenvironment as well as mapping active tissue forces.

Synthetic 2D substrates

Bio-engineered 2D surfaces are the most commonly used assays to study epithelial mechanics as they can be fabricated with straightforward and mature microfabrication methodologies, e.g. clean room-based subtractive manufacturing and soft lithography³⁵, and are compatible with optical imaging. These include the methods for patterning ECM adhesive/nonadhesive cues³⁶ for controlling epithelial assembly^{37,38}, introducing micro-/nano-scale topographical features^{39,40}, and generating stiffness gradients²¹. The synthetic substrates thus provide reductionist conditions with the independent control of individual spatio-temporal parameters, such as biochemical cues, tissue organization, spatial geometry/confinement, and substratum viscoelasticity, that are largely entangled *in vivo*. Further, these techniques can be used in a combinatorial manner to produce even higher levels of complexity in both 2D and 3D. We do not intend to exhaust the microfabrication details as they have been addressed elsewhere^{35,41-43}, but will focus on the important development of artificial substrates that reveal insights of epithelial mechanics.

Surface patterning of epithelial layers

To study tissue mechanics, a simple epithelial monolayer can be assembled on a flat substrate by growing them on both non ECM-coated surfaces such as surface-treated, hydroxyl-rich polystyrene⁴⁴ or ECM-coated surfaces⁴⁵ *in vitro*. One conventional way to study epithelial collective migration is to observe how epithelial cells expand into free space. A canonical assay is to create free edges in a confluent epithelium known as the “scratch assay”⁴⁶ that employs a pipette tip to remove stripes of cells (Table 1 – Scratch assay). While being cheap and convenient, it offers poor control over the geometry of the boundaries and can cause unwanted biochemical signaling due to cell death. To overcome this limitation, another wound healing model allows better control of boundary conditions by using elastomeric membranes or polymer slabs as obstructions of defined shape that are peeled off after the epithelial layer has grown to confluence beside it⁴⁷⁻⁴⁹ (Table 1 – Model wound assay). As cells are initially prevented from growing under the obstructions, this leaves a pristine empty edge of controlled geometry without the remnants of cell debris and cell-modified ECM^{50,51}. Another way to create gaps in the monolayer is to introduce laminar flows of protease trypsin-containing solutions in microfluidic chips to locally remove cells in the microchannels^{52,53} (Table 1 – Microfluidic assay).

Besides the regulation of the epithelial free edge, the ECM components^{45,48}, the overall geometry and confinement of epithelial layers^{11,29,30,54} also have strong impacts on tissue dynamics. Thus, one can assemble cell-adhesive biomolecules and/or cell-repellent chemicals on the surface³⁶ to guide cell/substrate

interactions. Biomolecular patterning (Table 1 – Patterning tissue on planar substrates) is achieved by several methods, including micro-contact printing (μ CP) using elastomeric micro-stamps^{43,54,55}, micro-stenciling by shadowing uninterested areas with masks and back-filling with protein⁵⁶, and dip-pen nanolithography^{57,58}. The bio-functionalization of proteins and peptides onto surfaces commonly involves non-covalent adsorption⁵⁶ or assembling bio-cross-linkers⁵⁹ for chemically binding, such as click chemistry⁶⁰, N-hydroxysuccinimide ester reaction⁶¹, or hydrogen bonding⁶². Additionally, the nanometer-scale control of spatial distribution of cell-adhesive ligands on flat surfaces can be achieved with block copolymer micelle nanolithography^{63,64}. In such method, the separation between each gold nanodot-anchored integrin ligands is fine-tuned by the molecular weight of the diblock copolymers and thus, enabling high precision in regulating loading force per adhesive site and relevant mechanosensing⁶⁵. To better mimic *in vivo* conditions such as the modeling of neighboring cell-substrate and cell-cell adhesion, multiple types of proteins need to be patterned closely at high spatial resolutions^{66,67}. This can be done conveniently using digital projection array systems with deep UV degradation of biopassive polymers that allows for the backfilling of proteins in selectively exposed regions⁶⁸⁻⁷⁰ (Table 1 – UV patterning). Bio-printing on 3D surfaces^{66,67} or creating switchable adhesive substrates⁷¹ whose adhesive properties vary in time or with light exposure can be done by combining the above-mentioned techniques. These advances constitute the next step towards the fabrication of active adhesive substrates with geometry and topology reminiscent of physiological situations.

Microengineering substrate elasticity and viscoelasticity

In vivo, stiffness patterns dictate collective cell migration such as that of neural crest cells during *Xenopus laevis* morphogenesis²⁰ or glial movement in drosophila development⁷². The development of *in vitro* substrates with defined variations in stiffnesses allows the in-depth understanding of tissue stiffness sensing processes. The most commonly used materials for such purposes include stiffness-tunable continuous substrates such as soft silicone substrates and plastics (polydimethylsiloxane (PDMS)⁷³ and polyvinyl alcohol (PVA)⁷⁴) or hydrogels (polyacrylamide (PAA)^{64,76,77}, polyethylene glycol (PEG)⁷⁷, hyaluronic acid (HA)⁷⁸, and collagen⁷⁹). The substrates' mechanical properties can be altered by varying the degree of crosslinking⁵⁹. Importantly, the properties of some materials such as PAA, are univariate elastic spanning stiffness from 0.1 – 200 kPa, while others including PDMS can switch from a predominantly elastic regime at high cross-linker content to a more viscous one at low cross-linking density⁸⁰. Thus, special attention needs to be paid to the viscoelastic properties of the material as elasticity and viscosity may lead to distinct cell reactions^{80,81}. For example, epithelial monolayers have been found to form multicellular gaps on viscous but not soft elastic gels⁸². Recently, a PAA gel with independently tunable viscosity and elasticity was synthesized by grafting linear dissipative elements into an elastic PAA network⁸³ (Table 2 – Engineering substrate elasticity and viscosity) thus allowing the precise mimicking of tissue viscoelasticity.

Similar to synthetic polymers, the matrix stiffness of naturally occurring biopolymers, such as collagen and fibrin, can be tuned by changing the protein density⁸⁴ and incorporating other proteins⁸⁵. For collagen, the matrix mechanical properties are also related to other variables, e.g. pH and polymerization time, during polymerization reaction⁸⁶. Further, the nanoscale rigidity of collagen fibrils can be modified with a dehydration treatment⁸⁷ and the matrices can be strengthen by cross-linking reducing sugars into the network by the Maillard reaction, i.e. glycation^{88,89}. Interestingly, the latter allows to modulate collagen stiffness without much interference in gel density and fiber architecture⁸⁹ and further, glycated ECMs are thought to link to the development of a series of disease states, like diabetes⁹⁰ and cancer⁹¹. On the other hand, in

contrast to elastic synthetic polymers, one should pay special attention to the fact that most natural biopolymers are both elastic and plastic. For instance, in previous rheology studies, collagen gels show a linear elastic response below a stress/strain threshold and beyond that their elasticity becomes non-linear⁹², exhibiting stress relaxation⁹³ and history-dependent plasticity⁹⁴. In several models⁹³⁻⁹⁵, unbinding, resurging, and sliding of weak cross-links between collagen fibers account for such effects as covalently strengthened networks diminishes the relaxation⁹³ and a higher collagen concentration enhances the plastic deformation⁹⁵. Though the chemical nature of the processes remains elusive, several weak interactions, including hydrogen bonds, electrostatic and hydrophobic interactions^{93,96}, have been proposed to contribute to the collagen plasticity. Thus, while nature biopolymers offer a milieu closed to physiological conditions and tunable properties, their plasticity allows cells to remodel the gels and cause irreversible deformations with traction forces, suggesting it an important determinant of cellular mechanosensitivity.

Another level of complexity involves the spatio-temporal control of surface stiffness (Table 2 – Engineering substrate elasticity and viscosity), for example through the control of the distribution of substrate crosslinker densities by diffusion⁹⁷⁻¹⁰⁰, temperature gradients^{73,74}, and patterned photopolymerization^{75,101}. For instance, a PAA gel with linear stiffness gradients was generated by differential UV-irradiation of a photo-sensitive initiator which enabled the study of epithelial durotaxis²¹. However, the variations in porosity⁹⁸ and surface chemistry⁸¹ of the gel are not fully independent of the changes in crosslinker densities, and the poor reproducibility is still an existing challenge for UV photopolymerization⁷⁶. Another way to fabricate stiffness patterns in continuous substrates is to produce hybrid materials by grafting soft gels on rigid patterned surfaces of different height distributions^{102,103} (Table 2 – Compliant soft gel layer). In these cases, regions on top of the soft gel closer to the rigid surface will be stiffer independently of gel pore size and surface chemistry. Other than continuous materials, discrete substrates of different stiffness can also be fabricated in the form of micropillars¹⁰⁴⁻¹⁰⁶ (Table 2 – Pillar arrays). Apart from the above techniques (For a summary of advantages and disadvantages of these techniques, the reader can refer to Table 2 – Engineering substrate elasticity and viscosity), which are starting to become more widely used, innovations in 3D-printing and multiphoton lithography^{107,108} are anticipated to lead to further advances in this field and have been used to precisely control the elastic modulus of 3D materials for example.

Patterning nano- and micro-topographical features

Topographical features ranging from nano-fibrous ECM networks to surfaces with micron-scale out-of-plane curvatures are constantly present in the microenvironment of epithelia, such as those seen in the villi and crypts of intestinal gut surfaces and capillaries of kidney nephrons. Among such structures, multicellular epithelial tubes which are cylindrical in shape are ubiquitously found. To replicate a curved cylindrical substrata, some readily available laboratory materials such as glass capillaries¹⁰⁹ and metal wires¹¹⁰, can be used as templates for molding. For capturing other more complicated epithelial structures, researchers have taken resort to soft lithography methods³⁵ (Table 2 – Engineering substrate topography). This class of methods, whose lateral resolution is limited by the wavelength of the exposure beam⁴¹, facilitates the manufacturing of micro-architectures of not only the more routine rectangular structures but also those with surface curvatures. For example, villi-shaped PDMS and hydrogel micro-architectures have been produced to mimic the intestine^{31,111}, while the fabrication of micropost arrays can be used as obstacles in the path of an epithelial expansion³⁹. Additionally, topographies on the scale of submicrometers have shown to impact multiple cellular behaviours^{112,113}. To deposit secondary micro-topography on a curvilinear substrate¹¹⁴, for instance, one can employ an extended version of soft lithography¹¹⁵ to transfer micro-features with

deformable and compliant stamps. The production of microscale topographies can also be achieved *via* means of laser ablation^{116,117} and 3D-printing¹¹⁸ (Table 2). These techniques are versatile but often require nontrivial refinement of the instrument to increase the resolution and throughput. On the other hand, the smooth substratum can be turned into fibrous textures by coating with micro/nanofibers using electrospinning¹¹⁹ (Table 2 – Electrospinning). Electrospun polymeric fibers of defined diameters can be laid out in a completely random or highly aligned fashion – two different organizations of fibrous ECM that can impact on epithelial metastasis¹²⁰ and development^{3,22}.

3D hydrogels

The aforesaid synthetic substrates are usually considered as 2D cell culture as cells on such substrate encounter with adhesive cues that are only accessible from one side (Table 3). This configuration pre-defines the axis of cell polarity that is perpendicular to the surface. However, geometric complexities can be included by patterning large topographic features of cell-comparable dimension, such as pillars and wells, on a flat surface^{31,111}. Such substrata can mimic aspects of specific epithelial morphologies, e.g. the 3D intestinal villus-crypt axis^{31,111} (Table 3). On the other hand, to better explore the effects of the 3D microenvironment *in vivo* on tissue behavior, where tissues are presented with ECM on all sides, cells can be embedded in 3D ECM materials and biomimetic gels (Table 3). Hydrogels are widely used for mimicking the ECM and there are three types – one derived from natural sources by the process of decellularization, such as Matrigel^{TM121} and collagen I¹²², synthetic hydrogels such as PAA and PEG, and the hybrid of these two. The naturally extracted hydrogels contain close-to-native fibrous architecture and are rich in proteins, ligands, as well as soluble factors, but these components have high batch to batch variations, weak mechanical properties, and inherent complications, like undesired immunogenicity and impurities^{123,124}. Furthermore, these native gels have properties such as ligand density and gel stiffness that are interdependent, thus the independent role of each factor cannot be studied separately. In contrast, man-made gels can be custom-designed and have stiffness, topography, degradability of the crosslinkers, and presentation of chemistries such as different adhesion peptides and growth factors that are more independently tunable¹²⁵. The embedded epithelia in hydrogel usually grow into spherical organotypic models with hollow lumens within polarized cell layers¹²⁶ (Table 3), while the malignant types form disorganized and nonpolarized cell clusters¹²⁷. This process shares many underlying principles with *in vivo* epithelial morphogenesis and neoplastic progression. Additionally, the system allows for convenient investigation with a number of biochemical factors to test the epithelial organoids^{125,126}, which are 3D stem-cell derived tissue constructs mimicking their corresponding organs. Despite being excellent *in vitro* models, the epithelial organoids have not yet been broadly pursued in the study of tissue mechanics, in part because that it relies on cell-driven self-assembly, which results in poor reproducibility in shape and composition, thus difficulties in quantitative analysis¹²². To overcome these limitations, the use of such gels can be combined with soft lithography techniques and be patterned into gel structures with precise 3D geometries^{122,128,129}. These hollow structures can then be loaded with cells to generate tissues of well-defined profile such as epithelial tubules (Table 3) to study processes including geometrically-induced cancer metastasis and mammary branching structures^{122,128}. When such cell-laden hydrogels are hung between two elastic micro-pins, this enables direct measurement of forces from 3D microtissues^{130,131}. Recently, different reversible chemistries have provided powerful approaches for independent control of ligand presentation, degree of crosslinking, and degradability to dictate cell fate³⁴. Hence, this advance constitutes the next step towards the 3D gel-based culture systems with spatiotemporal variations in property that capture the dynamic reciprocity¹³² between mature tissues of complex functions and their microenvironment.

Probing tissue mechanical properties

The passive and active rheological properties of cells and tissues often correlate with their physiological states and can be important for their specific functions^{6,36,133}. It is thus important to understand the rheological behaviors of the tissue under external perturbations or intrinsic cell forces in different microenvironments, and methods have been developed to probe these properties from molecular and subcellular, to cellular and tissue levels. The mechanical parameters that provide important information include deformation, rates of deformation or velocity fields, and traction forces that cells exert on the substrate and the intercellular mechanical stress. These parameters, when coupled with the cellular architectural information through imaging, helps to build a mechanistic understanding of the tissue rheology. We briefly summarize some of the techniques here important for studying epithelial mechanics, and refer the interested readers to an up-to-date review for a detail account of these technologies¹³⁴.

External perturbation of cells by nano- and micro-mechanical tools

To study tissue behavior under external perturbations, the cells must be subjected to mechano-probing by nano- or micro-mechanical tools. At the molecular and subcellular scales, such tools include the Atomic Force Microscopy (AFM)¹³⁵, magnetic^{136,137} and optical tweezers¹³⁸, and micropipettes¹³⁹, which provide kinematic and stress read-out from the deformation and movement of the probes on the one hand, and the information of the probe stiffness or physical field magnitudes on the other hand. AFM^{140,141}, one of the earliest tools used for such purposes, applies exogenous stress to cells locally through a mechanical cantilever with a sharp tip which serves for both topography imaging and viscoelastic property mapping¹³⁵. The AFM is a versatile system which can apply forces from the molecularly-relevant pN range up to hundreds of nN at the tissue level¹³⁴, and has been used to study tissue stiffness maps during epithelial expansion¹⁴² and even *in vivo* systems¹⁴³. Yet due to the physical attachment of the cantilever to the AFM scan-head, the system can have considerable mechanical noise, and can only be used to probe cells from the surface. Other techniques such as magnetic tweezers¹³⁶ and optical tweezers¹³⁸ can overcome these limitations by the delivery of tiny particles into the cell body, and the exertion of magnetic- and light-based forces on the order of pN – nN allow force exertion deep in the cell body without going through the cell surface¹⁴⁴. Magnetic tweezers have also been used to apply forces at the cell surface to study active single cell migration within an epithelium in response to forces¹⁴⁵ and to probe cell-cell junctions¹⁴⁶. To probe large scale tissue behaviors to external forces, mechanical stretchers, tissue-rheometers and force plates have been used^{13,147–150}.

Measuring internal subcellular dynamics and forces

Next, there are a variety of methods to measure the subcellular dynamics and endogenous forces relying on mechanical- or light-based methods. AFM probes are able to infer the apical epithelial tension¹⁵¹ and elastic modulus¹⁴². Further, light-based methods include the use of molecular tension sensors based on energy transferring principles of Förster resonance energy transfer (FRET)^{152,153} and nanometal surface energy transfer (NSET)¹⁵². These biosensors work by a distance-sensitive energy transfer principle involving two chromophores that are separated by a molecular tensor. The measurement of the energy transfer efficiency can be used to probe molecular forces specific to certain molecules of interest such as integrins at focal adhesions¹⁵⁴ and E-cadherin at adherens junctions¹⁵⁵. Also, the use of laser ablation allows the inference of relative tensions from the subcellular¹⁵⁶ to tissue-level¹⁵⁷ by measuring the immediate recoil speed of the

structures being cut^{133,158} which is important to understand stress anisotropy. Some of the techniques such as FRET and laser ablation can be used to study *in vivo* stresses but is invasive for the tissue.

Measuring tissue dynamics, forces, and structural information

Unlike the invasive nature in many methods for measuring subcellular properties, active dynamics and forces at the cell/tissue level can often be non-invasively inferred based on optical imaging of the tissue and the tissue-induced deformation of their substrata with pre-designed mechanical properties. In terms of tissue dynamics, each cell can either be directly followed in 2D or 3D by tracking their nucleuses, or a velocity flow field over the whole tissue can be measured by techniques such as Particle Image Velocimetry (PIV) or Optical Flow¹⁵⁹ (Supplementary information S1 (box)) based on naturally visible subcellular structures within the tissue. Further, to measure the traction forces that cells exert on their substrates in 2D or within a 3D tissue or gel environment, the synthetic substrate itself which provides the cells with the specific microenvironment conditions also acts as a force sensor, and are used in techniques such as the elastomeric micropillar arrays¹⁶⁰, traction force microscopy (TFM)¹⁶¹, or deformable particles that are inserted into tissues¹⁶². Again, common to these techniques, the local deformations of the substrates with respect to their rest state can be used to quantify the force fields acting on them if their material stiffness properties are known. For example, the in-plane cellular force-induced bending of discrete soft pillars can be measured by knowing the pillar bending stiffness, while the Young's modulus of continuous silicone matrices or hydrogels in TFM techniques are needed to infer stresses from the local matrix deformation quantified by the movement of embedded fiducial markers, assuming a homogeneous substrate material. Micropillars can only measure in-plane stress due to the high pillar stiffness in the direction normal to the surface on the pillar top, while TFM techniques can infer both in-plane and normal tissue stress on a 2D substrate. However, the cell-removal intermediate steps to generate a load-free state during TFM experiments are complicated and preclude any post-processing. Such problem has recently been addressed by electrohydrodynamic nanodrip-patterning highly regular arrays of quantum dots on elastomers¹⁶³, which offers a reference-free surface to deduce strain and stress in single cells as well as cell assemblies^{163,164}. Notably, there have been recent advances in inferring 3D traction forces of cells¹⁶⁵ or tissues¹⁶⁶ embedded in 3D gels, but the difficulties lie not only in the need for heavy computational methods but also in the heterogeneities of the gel arising in part due to irreversible deformations of the gel induced by cellular forces.

The mechanical stress within tissues is different from the traction forces that cells exert on substrates, but both quantities are ultimately linked by force balance and Newton's laws. Based on this idea, in 2D epithelial sheets, intercellular stress can be inferred from TFM data with additional assumptions of the epithelia. One such inference methods, i.e. Monolayer Stress Microscopy (MSM)¹⁶⁷, makes assumptions on the rheology of the epithelia, where the tissue is treated as an elastic material even on long time scales, while another method, i.e. Bayesian Inference Stress Microscopy (BISM)¹⁶⁸, circumvents this need by using a Bayesian statistical model and assuming a Gaussian noise in mechanical stress determination. While these 2D stress inference methods require the use of an *in vitro* environment, other reference methods are based solely on cell geometrical information from imaging¹⁶⁹, with assumptions about the relations between different mechanical stress components such as cell-cell interfacial tension and cell body pressures and can be applied for relative stress inference *in vivo* such as in the drosophila wing¹⁶⁹. We refer interested readers to a more detailed review of different 2D epithelial stress inference methods¹⁷⁰. For tissue stress inference in 3D, liquid oil droplets or soft polyacrylamide microbeads of known mechanical properties can be coated with adhesion proteins and be uptake by embryos or *in vitro* cell clusters to act as 3D force sensors¹⁶². Due to the

incompressibility of oil droplets, the isotropic part of the stress, i.e. mechanical pressure cannot be measured, which is a limitation overcome by the use of compressible polyacrylamide¹⁷¹ or alginate¹⁷² microbeads.

Living systems as active matter

The cellular rheological behaviors emerge from the ways that their molecular constituents react to externally or internally driven forces, which can be governed by molecular crowding^{173,174}, force resistant molecular interactions such as cross-linking of cytoskeletal networks¹⁷⁵, the internal energy injection by molecular motors³², and active mechano-transduction¹⁷⁶. At a larger length scale, tissue rheology is determined not only by the stress-strain behaviors of their cellular building blocks but is also highly dependent on the cell-cell adhesion strengths^{177,178}, and active cellular events such as cell division and extrusion¹⁷⁹. Such rheological behaviors are complex and depend on factors such as the time-scales that the biological material is probed, the magnitude and type of mechanical stress, e.g. stretch or compression, and the active behavior of cells^{173,174,180,181}. Also, when cells and tissues interact with the microenvironment, the active forces that they exert on the substrate and on each other allow them to migrate and undergo dynamic processes¹⁸². Below we discuss the material properties and active behaviors of the cell monolayers from the molecular to tissue level.

Molecular complexes and networks

The cytoskeletal proteins, i.e. actin, microtubule (MT) and intermediate filament (IF) endow the cells with their mechanical properties. Among these three types of proteins, actin is the most abundant, and the actomyosin network contributes significantly to the active, dynamic mechanical response of the cell^{32,183}. Reconstituted *in vitro* actin networks allow the study of single component systems with their molecular motors and have contributed significantly to our understanding of their mechanical properties. Cross-linked, isotropic networks¹⁸⁴ behave as viscoelastic gels^{18,32,185} with elasticities that can vary in the ranges from less than one to hundreds of Pa depending on filament lengths and cross-linker density¹⁸⁶⁻¹⁸⁸. Such gels portray strain-stiffening properties that could be due to microstructural non-linearities of single filaments behaving as semiflexible polymers^{186,189}, or could be due to network properties such as steric hindrance from cross-linkers¹⁷⁵ and reorientation of fibers into more aligned domains under stress¹⁹⁰⁻¹⁹². Owing to strain-stiffening effects, molecular motors which produce active stress/strain can enhance network stiffness up to 100 fold^{18,193}, and thus could help cells to stay intact when being mechanically stressed in the body. At longer time scales around a few minutes, the cytoskeleton networks can flow under stress and display viscous properties due to filament and cross-linker turnover (such as treadmilling of actin) and active forces that destabilize the network¹⁹⁴⁻¹⁹⁶. Large enough active forces can even fracture uniform networks to generate fluctuating and/or growing clusters of dense filaments interspersed among sparse regions¹⁹⁷⁻¹⁹⁹. In a network with higher filament density and cross-linker densities, and filament lengths, the network can acquire a nematic state with aligned filaments^{184,200,201}, which can confer anisotropic mechanical properties to the network.

Cell signalling and mechanical forces

Within cells, mechanosensing protein complexes and networks are able to respond to environmental inputs by triggering various signaling cascades. These include mechanotransduction machineries that allow force-

dependent gene regulation by transcription factors such as Yes-associated protein (YAP) and β -catenin at cell-cell junctions, and force-activated signaling due to the more recently discovered Piezo mechanosensitive ion channels (Figure 1). YAP (Figure 1a), which is first discovered as an important effector of the Hippo pathway that controls organ growth, is also found to be mechanosensitive²⁰². Under mechanical conditions such as fluid shear, large available spreading area, enlarged focal adhesions (Figure 1a-i, for a detailed introduction to focal adhesions, please refer to the section “Cell-substrate adhesion” below), and stiff ECM that promote large mechanical forces (Figure 1a), YAP is found to be activated and undergoes cytoplasm-to-nucleus translocation to activate gene transcription (Figure 1a-ii), leading to increased cell proliferation, while the opposite happens under high confinement and soft ECM conditions leading to YAP deactivation and cell death. Interestingly, the mechano-response of YAP may or may not be related to the Hippo pathway, in relation to its upstream kinases, MST and LATS²⁰³. Although cell-substrate and cell-cell adhesion-induced focal adhesion kinase (FAK)-Src pathway^{204,205} and E-cadherin homophilic binding²⁰⁶ respectively control YAP localization through the Hippo pathway, situations of high cell tension can dominate over it. For example, LATS inactivation which should in-principle increase the shuttling of YAP into the nucleus, does not have the predicted effect on cells experiencing low mechanical stress²⁰⁷. Indeed, high mechanical stress from actin stress fibers is found to be necessary to compress the nucleus and enlarge nuclear-pores for YAP to enter the nucleus (Figure 1a-ii), confirmed by AFM studies²⁰⁸.

Next, the β -catenin is a central player in the canonical Wnt-beta-catenin pathway that regulates cell proliferation and differentiation, well studied in the intestinal crypt stem cells²⁰⁹. In this pathway, the Wnt protein which is a growth factor, triggers the pathway to inhibit the degradation of β -catenin²¹⁰. This allows the translocation of β -catenin into the nucleus to act as a transcriptional coactivator. Apart from its transcriptional role, since β -catenin is also a structural molecule for the AJ formation, E-cadherin-mediated cell-cell adhesion in a collective cell situation sequesters β -catenin at the cell-cell junctions (Figure 1b-i), and is thought to be a negative regulator of the Wnt pathway^{211,212}. In the absence of physical strain, extra β -catenin in the cytoplasm other than at the AJs is proteasomally degraded (Figure 1b). However, it was found that stretching the epithelium causing high tension at the AJs allows the displacement of β -catenin from the AJs into the nucleus, leading to cell cycle re-entry and increased cell division²¹³ (Figure 1b-i). Last but not least, the Piezo mechanosensitive ion channel^{13,150} is a class of transmembrane proteins that are activated by membrane stretching due to various mechanical stimuli (Figure 1b-ii) to let in ionic currents and trigger signaling pathways such as Ca^{2+} -mediated pathways (e.g. ERK1/2-dependent transcription of cyclin B, Figure 1b-ii). Piezo proteins are found in multiple organs in the body and help to sense blood shear flow, regulate cell density under homeostasis, and detect sound-generated vibrations among other functions. In short, the different molecular mechano-sensors could play overlapping roles to ensure a robust mechano-signaling program. In the following section, we discuss the upto-date mechanical insights of cellular responses to external mechanical stimuli at cell-substrate adhesion/cell-cell cohesion.

Cell responses to mechanical stimuli

Similar to strain-stiffening in reconstituted networks, stretch-induced stiffening, dependent or not on actomyosin activity, has been seen locally or over a whole cell in microplate or stretchable membrane manipulations^{214,215}, yet, the rheological behaviors and mechanisms of cells are more complex than the reconstituted ones. Time-scales are important, as cells have been found to obey “passive” viscoelastic response at short times (seconds to minutes) in uniaxial step-stretch and micro-rheological measurements^{181,216}, and exhibit a further active reinforcement of their actin-dependent traction forces and stiffening at longer times upon stretch (up to one hr)¹⁸¹. Consistent with the idea of active reinforcement, AFM measurements found a softening of cells in the same time frame upon inhibition of myosin motor

activities²¹⁷. Apart from stretch, compression also induces a stiffening of cells which can be related to an increasingly crowded subcellular environment, as found in osmotic compression experiment¹⁷⁴. In reality, cells can even portray a strain-softening behavior in their micro-rheology within seconds of a step or oscillatory stretching before (or simultaneously with) stiffening or resolidification^{173,218}. Softening was attributed to a fluidization of the cytoskeleton in analogy to that observed in passive, crowded granular materials, and could operate at shorter time-scales and at higher strains (> 10% in the cell), and depends on the pre-stress in the cell¹⁷³.

Cell-substrate adhesion

Due to their internal activity, tissue cells can intrinsically generate local contractile stresses in the cell body causing their lengths to contract²¹⁹. When adhering to a substrate which may resist this self-contraction, cells are able to spread and actively regulate their own mechanical phenotype. Within cellular monolayers, cell adhesion comes from both interactions with the substrate and adjacent cells. Cell-substrate adhesion is coordinated through integrin-based complexes called focal adhesions (FAs, Figure 1a-inset) which undergo a force-dependent maturation to allow cells to sense the mechanical properties of its microenvironment such as the substrate stiffness. Broadly speaking, there is a positive feedback mechanism at the molecular level mainly due to mechanosensitive molecules that allow FAs to grow in size on a stiffer substrate by sensing forces^{220–222} (Figure 1a-i). For instance, talin increases its adhesion infinity to the F-actin linker protein under force, i.e. vinculin by unfolding and revealing a cryptic binding site such that more F-actin can bind to the growing FA (Figure 1a-inset). However, the simplistic view that FAs increase monotonically on stiffer substrates has been challenged by the ‘molecular clutch’ model that posits biphasic modes of force regulation in response to substrate stiffness needed to match the net binding rate of integrin molecules or protein complex growth rate to stabilize FA structure to ensure proper adhesion^{223–225} (Figure 1a-inset). Further, the model proposes a maximum threshold in the reinforcement of FAs, which is caused by the finite size of FAs and thus, on rigid substrates with high ligand spacing, the FAs would collapse when the loading force per integrin-ligand bond is beyond the threshold⁶⁵. *In vivo*, for cells to make an adhesion connection to the surrounding, there are different types of ECM proteins, such as fibronectin, collagen and laminin that require the binding of different types of integrin molecules at the cell-substrate interface. It was found that these different ECM-integrin binding partners induce different traction force levels in cells *in vitro*¹⁶, thus suggesting that the threshold of mechanical responses can be tuned by the different combinations of ECM proteins and the integrins they engage.

Together with the local mechano-regulation through FAs, the mechano-active behavior of cells can occur at the whole-cell scale through actomyosin remodeling. Contrary to passive materials, active stresses are generated within the cells in response to mechanical stimuli that include the application of external forces²²⁶ or changes in substrate stiffness¹⁹. For instance, actin stress fibers can coarsen under larger forces²²⁷ and even promote transition from an isotropic, i.e. on soft substrates, to a nematically ordered, i.e. on stiff substrates, as the active stress is proportional to local ordering of actin filaments^{19,106}. This view has been described at the single cell level but may be extended to cellular monolayers since multicellular scale force transmission is necessary to explain collective cell behaviors. Actin-based mechanical link across cell-cell junctions can thus serve as a template to promote large scale polarized cellular clusters²²⁸.

The dynamic and mechanosensitive cell-cell adhesions

When cells assemble to form a tissue, different types of adhesion complexes, i.e. tight junctions (TJs), AJs, desmosomes, and gap junctions form at the cell-cell junctions with specialized roles and different spatial localizations¹. The dynamic AJs are positioned close to the apical side below the TJs and consist of the transmembrane classical E-cadherin that links to the F-actin allowing for junctional remodeling^{229,230} (Figure 1b-inset). At the same time, they are the main junctions that maintain a dynamic tissue-level cohesivity by sustaining normal levels of mechanical tension throughout the tissue, giving rise to a tissue-level elasticity of few hundred Pascals as measured by AFM indentation¹⁸⁰. At these junctions, cell-cell adhesion complexes and the actin cortex contractility interplay (Figure 1b-inset) to produce an effective junctional surface tension²³¹ that provides an energy barrier to constrain the relative positions of juxtapositioned cells²³². These junctions are viscoelastic with molecular forces measuring up to hundreds of pN in *Drosophila* embryos using optical tweezers¹³⁸. The applied tensions readily equilibrated within seconds, consistent with the idea that these junctions are dynamic and can remodel under force. One main reason for the robustness of the AJs is that they can be actively strengthened under force through an α -catenin-dependent mechanism. The α -catenin acts as a mechanosensor that unveils its cryptic binding site to vinculin upon 5 – 10 pN of forces, such that vinculin can bind and recruit another F-actin to reinforce the link at AJs^{137,233,234} (Figure 1b-inset). Due to the variability of two neighboring cells on both sides of the cell-cell interface, it can be difficult to study the role of such cohesion. To overcome this complexity, *in vitro* systems can present cell-cell adhesion proteins on vertical walls to cells that can mimic cell-cell contact in single²³⁵ and collective cell conditions⁶⁶. These approaches have been shown to reproduce certain important aspects such as the polarization of proteins at the cell-wall interface.

Active tissue dynamics driven by stresses and other mechanical factors

Not only do single cells demonstrate active mechanotransaction, but cells in a monolayer also actively, reciprocally interact with the substrate and show a tug-of-war balance with other cells and thus receive forces from their neighbors through cell-cell adhesions. The emergent mechanical stress distribution from these cellular processes in the tissue leads to local spatial stress gradients that drive local movement of groups of cells and/or cell body deformations (strain) with respect to the local emergent and actively tunable material properties of the tissue. To understand the tissue dynamics, the experiments are done in close contact with theoretical modeling and there are two types of approaches – agent-based and continuum modeling methods (Box 1). We first talk about the tissue behavior under an overall extensile force, then its emergent behavior due to the active behavior of each of its cells which are interacting with each other.

Tissue mechanics and rheology under external forces

Similar to single cell rheology, tissue behavior in response to forces is complex and depend on the time-scales and strain magnitudes imposed on it (Figure 2a). At small deformations and fast rates on the order of seconds, the tissue rheology is thought to be largely dependent on the deformation of its constituent cells, as observed in experiments that involved the shearing of 3D cell aggregates or the stretching of suspended epithelial monolayers^{180,236}. Consistently, fast, oscillatory tissue perturbations in these experiments reproduced the fluidization effects as seen at the level of single cells. If large deformations are incurred at such short time scales which does not allow the cell-cell junctions to remodel in time, suspended monolayers can undergo tearing at the intercellular junctions when stretched to more than twice their original lengths¹⁸⁰ (Figure 2a-i). The idea that cell-cell junctions are the points of initial failure can also be seen in the hydraulic

fracture of tissues when epithelial tissues on hydrogels are stretched and compressed in succession which lead to hydrodynamic pressure accumulation in the porous gel beneath the epithelium²³⁷ (Figure 2a-ii). When epithelial tissues are stretched more slowly, the tissue can remodel to accommodate to the mechanical stresses in several ways. Other cell-cell rearrangements such as T1 transitions (i.e. the abolishment of an existing cell-cell contact and the creation of another involving two different cells) can give rise to a tissue-level viscosity that scales with the intercellular cohesivity¹⁷⁷ (Figure 2a-iii). Such cellular rearrangements are involved in many development morphological changes including the reshaping of the *Drosophila* pupal wing²³⁸ and *Drosophila* embryo germ band extension²³⁹. Further, when cell divisions occur in the direction of tissue stretch, this can relax the mechanical stress in that direction and promote epithelial homeostasis^{149,240} (Figure 2a-iii).

Nematic organization and mechanical stress

Although the tissue dynamics is chaotic with a highly heterogenous stress field, cellular monolayers can be seen as nematic tissues in some situations arising from the underlying elongated cell shapes (Box 1). This structure serves as an organizing principle for the understanding of the tissue flow field and stress distributions. As in other molecular nematic systems, anisotropically shaped cells including epithelial and fibroblastic cells tend to align with their neighbors in packed environments, yet distortions of these well-aligned and ordered cell regions frequently occur in the epithelium that can lead to bending or splaying (Box 1) of the cell bodies, and more excessively defects in the alignment of cells with undefined order^{29,241,242} (Box 1). This is clearly in contrast to an inanimate, passive nematic system where the formation of such orientational defects are unfavored due to high energy cost. Such defect regions are termed topological defects, where topological considerations allow defects to be grouped into distinct classes quantified by half integers (Box 1). In many cell systems, only two main classes of defects are found, i.e. the comet and triangular-shaped cellular arrangements^{29,241,242} which can be attributed to these defects having the lowest possible mechanical energies²⁴³. Despite the formation of the same arrangement patterns, the dynamics of such structures differ greatly between cell types. Epithelial or neural progenitor cells forming a comet arrangement (Figure 2b) tend to move in the comet-tail-to-head direction^{29,242}, while a comet formed from fibroblast cells usually flow in the opposite direction²⁴¹ (Box 1). It turns out that the continuous generation of defect patterns derives mainly from actomyosin activity that leads to active forces that amplify cellular fluctuations and distortions²⁹. Further, the specific motion of the comet defects is due to specific active forces patterns, that can be classified into two groups, i.e. “extensile” where force dipoles point outward from the long-axis of the cell body, or “contractile” with opposite force dipole directions (Box 1). Extensile systems generate comets that flow in the head direction, as seen in epithelial systems, while the opposite is true for contractile systems such as fibroblast collectives. It is unknown why epithelial cells behave as extensile systems when the underlying active force generation machinery is contractile. Apart from their interesting dynamical patterns, the high distortion and thus compressive stress localization at comet defects can lead to epithelial cell apoptotic extrusion and the triggering of YAP nucleus-to-cytoplasm translocation and deactivation²⁹ (Figure 2b). Conversely, triangle defects typically showed higher tensile stress and less extrusions.

Tissue organization and mechanical stress

Other than the topological defects, another geometry cue that can induce asymmetry and stress gradient development in the tissues is at the edges of the monolayer interfacing with empty regions. The absence of cell-cell contacts on one side of the cells at the tissue edge lead to the emergence of leader cells which are

highly motile and are with higher biochemical polarization cues such as Rac1 and integrin β 1, larger lamellipodia protrusion, and the ability to exert significantly larger traction forces than the follower cells^{49,244–246}. Multicellular “finger” structures emerge behind the leading cell, flanked by thick contractile actomyosin cables that constrain the overall movement of the follower cells with the leading cell²⁴⁵ (Figure 2c-i). In endothelial monolayers, the leading endothelial cell sends VE-cadherin enriched membrane protrusions from the cell-cell junction at its rear end toward the cell at the back²⁴⁷. The follower cell engulfs these ‘cadherin fingers’ and this confers an asymmetry at the cell-cell junction, thus relaying the polarity of the leading cell to the follower. Lamellipodial structures with polymerization of branched actin preferentially appear at open edges with a convex geometry, while pluricellular actomyosin cables connected through cell-cell junctions emerge more at concave geometries^{50,248} (Figure 2c-ii), although the molecular mechanisms that trigger one mode of actin force generation process over the other is yet unclear. As the first cells at the tissue edges are pulled forward, these mechanical strains undergo a periodic, wavelike propagation into the epithelium^{10,249} (Figure 2c-iii). It has been shown that mechanical stretching of cell-cell junctions correlates with the displacement of a known tumor suppressor protein, merlin from these junctions³⁷, thus allowing Rac1 reactivation and formation of ‘cryptic’ lamellipodia in the cells at the back (Figure 2e-iv). The repetitive mechanical wave propagation into the epithelium within few hours could thus trigger cells to move opposite to the direction of the wave and facilitate epithelium expansion. Although the wave propagates in a single direction into the epithelial layer, it does not trigger a purely straightforward motion within the monolayer during epithelial expansion¹⁸². For instance, there can be vortex movement within the cohort (Figure 2c-v). Intriguingly, it was also found that the mechanical waves at ultra-long time scales during epithelial expansion exhibited elastic-like behavior, with an in-phase stress-strain oscillation^{10,250}, and this apparent elastic behavior could stem from cellular activities²⁵¹. Further, there are certain epithelial tissues such as the skin that are intrinsically elastic in nature, where the tissue can be pulled by cells on adherent regions to cover over non-adherent regions while sustaining huge tension^{36,133}. Apart from intercellular adhesion, the cell-substrate interaction is also important in dictating tissue mechanics. High levels of substrate adhesion supports tissue spreading while low substrate adhesion promotes the clumping of cell collectives⁴⁵. Despite the importance of firm cell-substrate adhesion, an optimum level is needed to promote high tissue dynamics. Whereas epithelial tissues *in vitro* are dynamic with the constant proliferation and annihilation of nematic defects²⁹, fibroblasts which are known to exert significantly higher traction forces indicative of higher friction with the substrate were found to evolve in a collective to a seemingly passive material state with low dynamics and a minimal number of defects in a packed colony²⁴¹.

Another important parameter for tissue behavior is cell density. At low density, epithelial cells are more fluid and can exhibit tissue oscillations under confinement or wave propagation during expansion^{249,252,253}. At high density, cells possess smaller FAs (Figure 1a-i) and lower dynamics as they are less likely to protrude cryptic lamellipodia (Figure 2c-iv) in a packed environment to migrate²⁵². Consistently, tissue oscillations and mechanical waves (Figure 2c-iii) are attenuated in tissues with high cell density. Cell density constitutes a natural parameter, together with cell activity and cell-cell or cell-substrate adhesion to define a possible jamming state for the tissue, in analogy to granular materials^{6,254,255}. Intriguingly, epithelial tissues seem to portray a universal geometrical relationship between the cell aspect ratio, cell shape variation and the jamming state²⁵⁶. In fact, cell density is an important parameter that the epithelium actively regulates to achieve homeostasis through cell extrusion and/or division processes. Indeed, a universal cell area distribution was found in confluent monolayers which is determined by the underlying cell growth and division process, where cell division probability monotonically increases with cell area²⁵⁷. The mechanical stress within the tissue was found to be a potent regulator of not only crowding-induced cell extrusion as mentioned above^{13,14}, but also increased cell division events at high tension in low density or mechanically

stretched tissue¹⁵⁰. Intriguingly, both cell density-triggered extrusion and division events depend on the same Piezo mechanosensitive ion channels^{13,150} (Figure 1b-ii), and one hypothesis for this dual role could be the differential localization of Piezos on the internal or outer cell membranes based on cell density. In turn, cell extrusions and divisions can not only influence cell densities, but can also fluidize the tissue¹⁷⁹ as extrusions can induce long-range flows toward the site of extrusion²⁵², while cell divisions can inject long-range extensile flows in a nematic tissue^{258,259}. In multilayered epithelial systems such as keratinocytes, cell division and extrusion are even found to be coupled, where divisions tend to locally fluidize the tissue and promote cell delamination that lead to skin stratification²⁶⁰.

Tissue behavior in a mechanical environment

During embryogenesis or cancer metastasis, soluble factors and the types of ECM protein are crucial parameters that determine the triggering of the onset of coordinated migration^{261–263}. Other than these factors, the mechanics of the microenvironment also greatly impacts tissue organization that include the response to changes in the “passive” ECM properties including stiffness, geometry and topography or to the application of external forces such as shear flows²⁶⁴. Below, we focus on the impact of ECM mechanical properties on cellular assemblies.

Stiffness of the microenvironment

It is clear now that the stiffness of the microenvironment, which depends strongly on the specific ECM composition²⁶⁵, correlates with or directly influences a myriad of physiological processes such as stem cell differentiation *in vitro*^{266,267}, wound healing²⁶⁸, and migration of cells during morphogenesis *in vivo*²⁰. Single cell behavior has been shown to respond to substrate stiffness both *in vivo*¹⁴³ and *in vitro*⁹⁹. Such interplay at the cell-substrate interface exhibit a tendency of most mammalian cells to undergo durotaxis and move from a softer to stiffer region on 2D surfaces^{269–271}, which is a process that can also depend on the type of ECM the cell is adhering on¹⁰⁰.

Cell collectives also respond to substrate stiffness in ways similar to those of single cells yet exhibit complex behavior. In wound healing assays on PAA gels of uniform stiffness, epithelial expansion becomes more efficient on stiffer substrates, as cell speed, persistence and directionality all increased within the monolayer²⁷². These behaviors correlated with the more directed lamellipodia protrusions toward the epithelial expansion direction, and cell-cell adhesion was crucial for the rigidity-dependence in coordinated cell movements. Further, epithelial expansion also exhibits durotaxis^{21,273}. Tissues are more sensitive to shallower stiffness gradients when compared to single cells (Figure 3a-i) as cell-cell junctions allow the transmission of forces across the monolayer to allow the whole epithelium to act as a giant cell²¹ (Figure 3a-ii). Along this line, traction forces measured by TFM at both ends of an expanding monolayer are shown to be equal. Thus, the tissue edges on the softer region will contract the substrate more than on the stiffer region, leading to a net shift of the center of mass of the epithelium toward the stiffer side and giving rise to durotaxis^{21,274} (Figure 3a-ii). Further, using gel substrates of various rigidities, an interesting mechanical memory of the substrate rigidity mediated by the YAP mechanosensitive pathway^{275,276} has been revealed. When the epithelium is first primed on stiffer substrates for few days, they can continue to exhibit higher migration speed, form larger FAs and retain nuclear YAP when moving on softer substrates, as if they were

still on stiff substrates²⁷⁵. The YAP-mediated mechanical memory also allowed stem cells to undergo osteogenesis on softer substrates if they were primed on stiff substrates before that²⁷⁶.

Another dynamic response of the epithelium to stiff substrates is to undergo the epithelial-to-mesenchymal (EMT) transition^{277,278}, where cells in a tight cohesion tend to scatter from each other thus promoting increased cell migration. Such behavior may be related to increased traction forces on stiff substrates that overcome cell-cell adhesion strength (Figure 3a-iii). EMT is dependent on the nuclear positioning of the transcription factor TWIST1 under stiff conditions²⁷⁸ and can trigger the E- to N-cadherin transition at cell-cell junctions²⁷⁹. An EMT-driven durotaxis is observed in neural crest migration during development *in vivo*, as these cells collectively migrate to the stiffening mesoderm region²⁰. The mesoderm stiffens due to the increasing cell density in a region beneath the mesoderm, where the density increase is due to a separate morphological process called convergent-extension. In the context of cancerous cells, the high rigidity of tumor tissues as measured by magnetic tweezers can trigger the formation of larger focal adhesions in cells, disrupt AJs and tissue polarity, activate the ERK pathway and potentially lead to cancer metastasis^{280,281}.

Most *in vitro* studies on the effects of substrate stiffness have been done on 2D surfaces, and have even inspired the design of soft substrates on the order of few kPa with stiffness gradients to control the movement of inanimate liquid droplets²⁸². Yet the *in vivo* microenvironment is largely 3D and may change the way cells sense the microenvironment parameters including stiffness. Below, we discuss the role of the microenvironment geometry on tissue behavior.

2D vs 3D microenvironment

Cells are constantly presenting in a confined environment *in vivo* as seen in the case of cancer cell invasion for example. Both 2D and 3D *in vitro* systems have been instructive in understanding the role of the degree and shape of confinement in regulating cell behavior. For instance, during epithelial expansion into free space in 2D, cells that are allowed to migrate into confined straight lines by μ CP with single-cell size width exhibited caterpillar-like backward-forward movement unlike cell movement in non-confined regions¹¹. The cells which are in confined lines also portrayed higher overall expansion speed. On the other hand, when a confluent epithelial monolayer is confined in a circular microcontact-printed 2D patch smaller than the size of the correlation length of the tissue, the whole tissue rotates in a solid-disk-like motion^{54,283} (Figure 3b-i), again showing that confinement can induce more orderly collective cell movement. On 2D, confined monolayers of different shapes usually have leader-like cells that preferentially extend their lamellipodia at sharp protruding edges where mechanical traction and intercellular stress are found to be the highest²⁴⁸ (Figure 3b-ii). Interestingly, many of these phenomena on 2D substrates have been observed in tissues embedded in the 3D gel environment. For example, cells do establish coherent rotational movement in 3D confined spaces in hydrogel which drives the formation of lumen-enclosing architectures akin to *in vivo* glandular tissues²⁸⁴ (Figure 3b-i). Also, sharp edges in a 3D confinement promoted cancer cells to invade into the surrounding gel from their normal host tissue, again due to geometrically-driven accumulation of high mechanical stress from the host actomyosin activity²⁸⁵ (Figure 3b-ii). Further, leader cells that emerge from tissues in 3D exert large forces on the gel that was crucial to pull the follower cells forward¹⁶⁶ (Figure 3b-ii), similar to their 2D counterparts. Such leader cells could be the same cells from the tissue or could be a different cell type as seen in the case of collective cancer cell dissemination initiated by the pulling action of CAFs, requiring heterotypic N- and E-cadherin interactions between cancer cells and CAFs²⁸⁶.

Although similarities in tissue behavior exist between the 2D and 3D microenvironments, there are also specific tissue responses to 3D gel. An important geometrical feature of the 3D microenvironment arises from the fibrous architecture of the ECM constituents. Cell dynamical behavior on such nano-fibrillar structures can be studied in 2D which facilitates imaging and quantification. Indeed, when cell clusters were allowed to expand or migrate on the surface of a collagen gel or topographically patterned, lined-nanogrooves on PDMS, tissue movement correlated with the direction of these lined structures^{287–289} (Figure 3b-iii). This can be attributed to molecular contact guidance leading to aligned actin stress fibers and FAs along the nano-lines at the cell basal membrane²⁹⁰. The collective expansion of cells on such nanogrooves were found to be more efficient both due to higher motion persistence and greater intrinsic speed²⁸⁹. In 3D ECM, single cell and leader cells in cell collectives were found to deform and realign the fibers surrounding them in the direction of the traction force, which promoted further cell migration along these aligned fibers¹⁶⁶ (Figure 3b-iii). The migration of cells along fibrous tracks is an important phenomenon *in vivo*, as CAF-mediated realignment of collagen fibers around tumor clusters in human prostatic and pancreatic carcinoma samples promoted cancer cell invasion into the ECM at sites where these fibers emanated radially from the tumor, while in contrast, cell invasion was blocked at regions with tangential fibers around the tumor²⁷ (Figure 3b-iii). Similar CAF-assisted, cancer cell migration along fibronectin fibers were also observed in *in vitro* systems²⁹¹.

Interestingly, experimental evidences show that microenvironments that induce more consistent cell movements preserved collective cell migration over single cell migration in 3D and *vice versa*. In a microfabricated model 3D microenvironment, EMT-transformed epithelial cells were allowed to collectively migrate into micropost arrays on 2D substrates that disrupted continuous movement. Within these microposts, cells close to the edge of the collective tissue started to scatter in single cell fashion and migrated more persistently, while expressing high levels of mesenchymal marker, vimentin³⁹. It was found that single cell scattering was most optimal within micropost spacing of 10 μm , which is the size of a single cell. Further, melanoma cells from the dermis *in vivo* tend to migrate as collective strands along aligned muscle fibers which promoted coherent movement, while some of these cells adopted single cell migration modes when moving on loosely connected fat tissue²⁹². Finally, clusters of cancer cells were found to switch to a collective migration mode from single cell migration in highly dense collagen networks *in vitro* that promoted cell jamming²⁹³. Similarly, less degradable hydrogel slowed down cell migration speeds, and allowed collective endothelial cell sprouting and proper angiogenesis, while single cell migration prevailed in lightly cross-linked and more degradable environments¹²⁹.

Out-of-plane curvature

Apart from the purely 2D or 3D geometries, surfaces with out-of-plane curvatures present a “2.5” D situation that is also an important class of geometrical cues. *In vivo*, such out-of-plane situations can be seen for epithelial tissues in 3D ECM forming a lumen or cavity within the tissue, or for epithelial monolayers covering corrugated substrates such as those in the intestine villi and crypt. The formation of these epithelial structures can be studied *in vitro*, starting from 2D or 3D settings, due to the active self-assembly processes of the cells interacting with the substrates, as widely seen in organ-on-chips. Both biological parameters such as cell polarity and the type of ECM, and mechanical parameters of the environment such as substrate stiffness, confinement and geometry interplay to determine the type of structures formed. For example, dense, confluent cells on 2D hard surfaces can produce cyst-like structures²⁹⁴ suggesting that confinement is important for this type of morphogenesis. Indeed, micropatterning experiments where few-cell colonies

of high spatial confinement portray enhanced lumen formation attributed to a mechanically-driven cell polarization²⁹⁵. Under such high confinement, a preferential positioning of centrosomes and transport machineries toward the cell-cell junctions to initiate lumengensis was observed. Further, cells on 2D soft gels which allow large deformations of the substrate can form a villi-like configuration²⁹⁶. In 3D gels *in vitro*, cells can also spontaneously generate lumens and maintain a consistent apical surface facing the lumen. The initiation of the lumen²⁹⁷ and the maintenance of the apical surface²⁹⁸ are both dependent on Cdc42-driven cell polarization. Further, the type of 3D gel ECM can determine the speed of cell polarization, which in turn governs the mechanisms of lumen formation. In particular, slow polarization in collagen induces a cell apoptosis-driven cavity initiation, while fast polarization in Matrigel abrogates the need for apoptosis in luminogenesis²⁹⁷.

In essence, the shape of the out-of-plane structures are initiated and maintained by a delicate balance of forces due to cell polarization and the microenvironment mechanics. The forces include osmotic pressure driven by ion pumps, cell-cell and cell-substrate adhesion strengths, intercellular stress and acto-myosin contractility^{67,299}. For example, MDCK monolayers on non-porous substrates form upward bulging cysts due to the accumulation of osmotic pressure beneath the monolayer maintained by a tight junction-mediated apical seal, which overcomes a weak cell-substrate adhesion patch³⁰⁰. It was also found that the interplay between acto-myosin and the intercellular stress drives the elongation of tube structures in the direction of lowest cellular stress⁶⁷. Further, the maintenance of stable, curved epithelial structures require the differential strength between apical and basal cell surface tensions and/or contractility in theory³⁰¹. On the other hand, corrugated surfaces on 2D substrates is thought to be initiated by cell division-driven pressure that induces substrate buckling in theory³⁰², and/or contractile forces which cells exert on soft gels seen in experiments²⁹⁶. Since the formation of out-of-plane structures depends on the self-assembly and interaction of cells with their substrates, it is not a well-controlled process. Thus, to directly study the effects of substrate curvature on cell behavior, rigid substrates with well-defined curvatures are fabricated. For example, when cells are seeded on the outer surface of a cylinder, it was found that there is a preferential alignment of the cell body with respect to the cylinder axis that is cell-type dependent.^{303,304} Theoretical work suggests that this phenomenon can be explained by anisotropic properties of the stress fibers and is dependent on whether the active contractility or the bending elasticity of the stress fibers dominated³⁰⁵ (Figure 3c-i). Unlike epithelial cells on cylinders, such cells in hollow tubes tend to align more with the tube long axis^{110,306}, and more so with increasing actin contractility³⁰⁶, showing that there is a difference between the positive curvature outside the tube, and negative curvature inside it. This is consistent with the observations that cells often preferentially spread on flat or surfaces with positive curvature i.e. domes, and not on surfaces with negative curvature in well-like structures^{307,308} (Figure 3c-ii). The reason for these observations could be that there is a bigger angle between stress fibers and a surface which is negatively curved, and the focal adhesions experience a larger upward lifting force which can detach them and the cell more easily as shown in modeling work^{309,310} (Figure 3c-i).

The collective effect of cells in a monolayer is also evident on curved surfaces. Even when single, isolated fibroblast cells do not align in the inner surface of a hollow tube with low curvature, a collective of such cells do align in a tube with the same radius under packed conditions³¹¹. This enhanced sensitivity to curvature due to the collective effect is not yet understood, but could be related to the emergence of a collective-level twisting mechanical energy that can in theory lead to unfavorable alignment of nematic liquid crystal particles in the short axis of a tube³¹². The type and extent of curvature also plays a critical role in the collective cell migration of an epithelial tissue within a hollow tube or on the outside of cylinders

along the long axis. High curvature in both situations has been found to promote cell detachment at the edge of the tissue reminiscent of the EMT process^{109,110} (Figure 3c-iii). Yet, negative and positive curvature do influence the speed of tissue migration as a function of magnitude of curvature in different ways. In hollow tubes i.e. negative curvature, epithelial tissue migration speed is enhanced as curvature is reduced, or in other words when the tube diameter is increased and intact cell-cell junctions are important for the observation of such behavior¹¹⁰, while it is the opposite for cylinders, as tissue expansion speed is reduced as curvature is reduced¹⁰⁹. Moreover, the proper balance of the cortical tension in a tissue may vary as the geometry of the monolayer changes from 2D planar to curved geometry. A recent attempt to reproduce intestinal epithelial villus-like architecture³¹ found that a tissue-level cortical contractility remains isotropic on flat substrate even when the AJs are impaired while epithelia conforming to local curvature require stable cell-cell junctions to balance the apical contraction. The lack of stable AJs then compromises epithelial integrity in 3D and causes the growth of tuft-like structures above the surface of the tissue (Figure 3c-iv).

Conclusion

By contrast with equilibrium systems, cellular systems including cellular monolayers belong to the category of out-of-equilibrium materials. Hence, large-scale dynamical patterns can emerge from the continuous energy injected by the cells themselves through molecular forces generated by interactions between molecular motors and the cytoskeleton. Macroscopic behaviors of biological tissues result from the integration of these subcellular active forces and a remaining difficulty in understanding collective cell dynamics both experimentally and theoretically relies on the coupling between these multiscale processes.

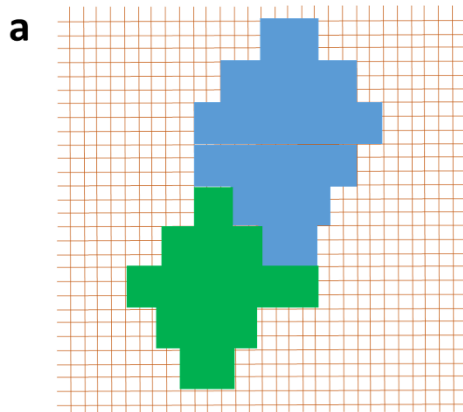
From a mechanical point of view, the emergence of large-scale structures observed in multicellular systems can be seen as a tug-of-war between forces exerted at the cell-substrate interface and at cell-cell junctions which plays a critical role in the regulation of tissue integrity. As active materials, cellular monolayers and their mechanosensitive structures do not only apply and transmit forces on their surrounding environment but also adapt and respond to physical cues including stiffness, geometry or topography. The mechanical properties of the environment can shape tissue organization by modifying mechanotransduction pathways and ultimately gene regulation. The recent discovery of the role of tissue stiffening on the coordination of collective cell migration *in vivo*²⁰ exemplify the importance of tissue mechanics to understand physiological processes and demonstrates that back and forth exchanges between *in vitro* and *in vivo* studies remain crucial for deeper understanding of biological processes.

As discussed in this review, future technical advances in engineering materials will mimic more complex environments closer to *in vivo* environments. The coupling between microfabrication techniques and advanced biochemistry will help us to understand the core mechanisms of physiological and pathological situations. Along this line, *in vivo* situations often rely on the interaction between various cell types that can be designed by engineering new environments. For instance, developmental processes such as dorsal closure of epithelial cells in *drosophila*³¹³ and gastrulation as well as tumor formation²⁸⁶ rely on active interactions between different cell populations. As such, the substrate over which cells are migrating *in vivo* can be composed of other cells that could in turn actively modify the environment. A new promising challenge at the interface between materials and cell biology would thus be to develop biomimetic active materials that could mimic complex biological interfaces.

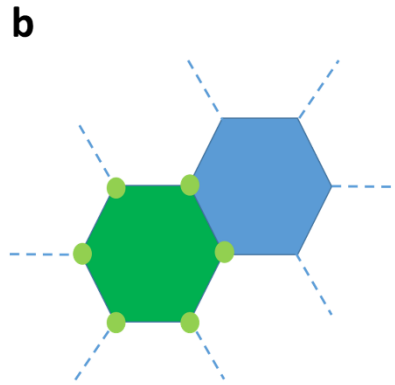
Acknowledgements

The authors thank group members from Mechanobiology Institute (MBI), Singapore and Institut Jacques Monod (IJM), Paris for helpful discussions. We thank Dr. René-Marc Mège from IJM for help at improving Figure 1 and the text in “Cell signalling and mechanical forces” section. W.X. has received funding from the People Programme (Marie Curie Actions) of the European Union’s Seventh Framework Programme (FP7/2007-2013) under REA grant agreement n. PCOFUND-GA-2013-609102, through the PRESTIGE programme coordinated by Campus France. Financial supports from the European Research Council under the European Union’s Seventh Framework Program (FP7/2007-2013) / ERC grant agreements n° 617233 (B.L.), Agence Nationale de la Recherche (ANR) “POLCAM” (ANR-17- CE13-0013), The Groupama Foundation – Research for Rare Diseases (D.D.), NUS-USPC program, The LABEX “Who am I?” and MBI, Singapore are gratefully acknowledged. C.T.L. and D.D. thank the support from the Human Frontier Science Program (RGP0038/2018). T.B.S acknowledges the support from the Lee Kuan Yew (LKY) Postdoctoral fellowship and Tier 1 grant from the Ministry of Education (MOE), Singapore.

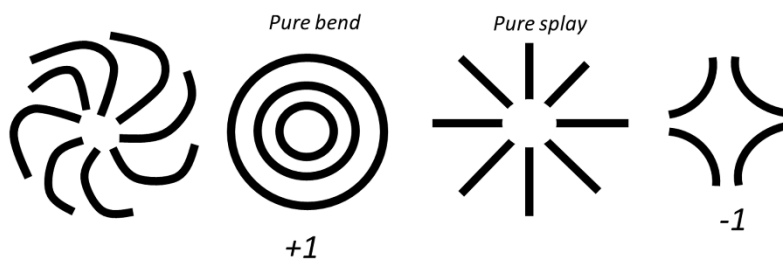
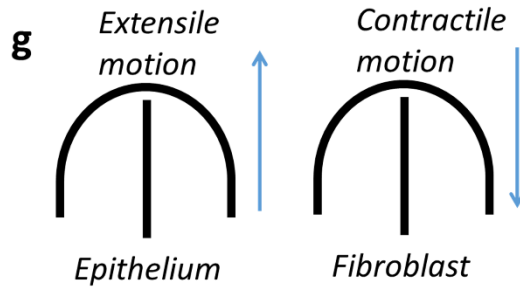
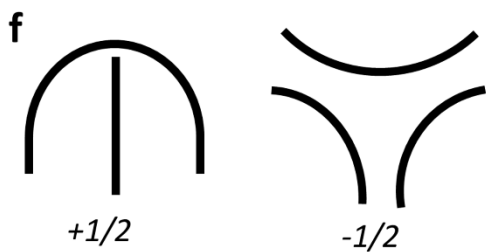
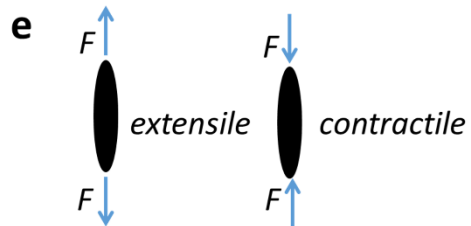
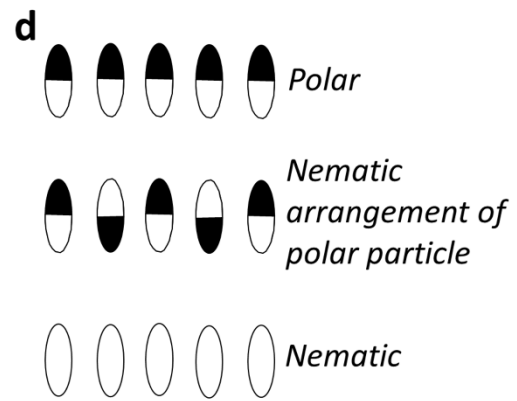
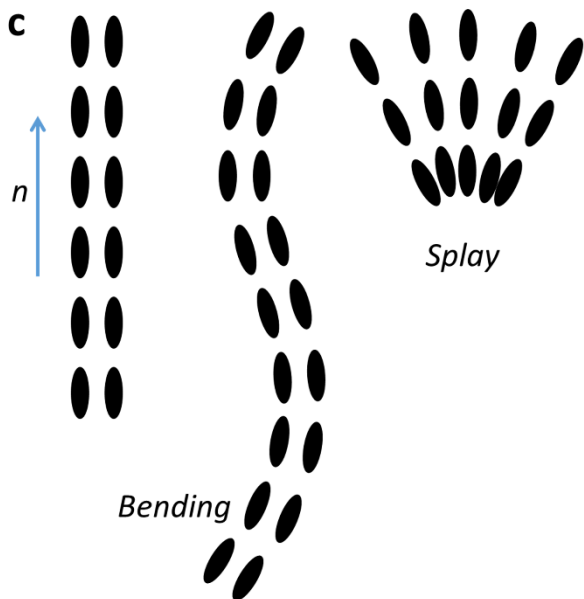
Box, Tables and Figures



CPM



Vertex model



Box 1: Theoretical Modeling

Theoretical modeling is increasingly important in cell biology to make sense of experimental results where the parameters are usually not fully controllable, and further make predictions and validate hypotheses. The modeling strategies used to understand the mechanics of the epithelium and collective cell dynamics can be broadly classified into two types i.e. agent-based and continuum models. In agent-based models, the individual agents can be explicitly simulated, and parameters such as the positions and velocities of the cells, as well as other local parameters such as the cell-cell adhesion strengths and cell shapes are crucial read-outs or ingredients of the models^{314–316}. Another advantage of agent-based models is that the properties and functions of individual agents can be actively and adaptively modulated in response to external chemical and physical stimuli as seen in experiments. One example is the possibility of studying the role of active junctional mechanics and contact inhibition of locomotion in epithelial response to wound³¹⁷. On the other hand, continuum models locally blur the details of individual agents by averaging over them and replace the many parameters found in particle-based models with a few mesoscopic variables such as viscosity and elastic modulus^{251,318}. Their origin derives from the many successful hydrodynamic and continuum elastic media theories. The advantages of continuum models over particle-based models in studying collective cell dynamics are that they simplify the numerical description of long-range movements and emergent properties, but it can be ambiguous to relate the local cellular parameters with these mesoscopic variables. Below, we briefly discuss different classes of such models most common to 2D epithelial monolayers, while more details of the modeling of collective tissue dynamics in general can be found in other reviews^{319–321}.

Agent-based models

One agent-based model used to describe epithelia is the cellular Potts model (CPM)^{315,316}. CPM is formulated on a fixed lattice, where an ensemble of lattice sites with the same state is considered a cell (Figure a). The bonds between two lattice sites are assigned an energy depending on the states of the lattice sites around it, such that there exists an energy cost when two different cells are side by side and the areas of single cells are constrained, among other rules. The energy of the whole system is the sum of the individual bond energies and the energy cost of individual cells deviating from their target cell areas, and the state of the system can be iterated by a Monte-Carlo algorithm to finally reach the lowest energy steady state possible. There are some shortcomings of the CPM such as unrealistic membrane fluctuations not observed in experimental systems³²². Another frequently used particle-based model is the vertex model^{158,314,323} which does not necessitate the use of a fixed lattice. Here, one interface of a cell is taken as a straight line between two points which are the vertices of cells, thus the cell assumes a polygonal shape (Figure b). The cell vertices are allowed to move and evolve according to equations of motion (thus the name of the vertex model), where the force acting on each of the vertices is the gradient of the local energy at each time point. The local energies comprise of a line energy describing the tension between the touching surface of two cells, an area energy describing the compressibility of the cell size, and others. Further a more recent development combined energetic terms from the Vertex Models with motile forces of cells to create Self-Propelled Voronoi (SPV) models where Voronoi tessellations used as the cell center motions are tracked in simulations²⁵⁴. With the addition of orientational feedbacks to align a cell's alignment with local average migration velocity, one can obtain a rich phase diagram with four distinct kinematic phases. Apart from the standard liquid and amorphous solids phases captured under low polar interaction strengths, a strong alignment feedback term introduces the emergence of flocking behavior as seen in collective cell migration³²⁴. The latter phenomenon has been used to describe the unjamming and increased collective migration due to the actions of RAB5A which is a key endocytic protein that promotes more traction forces and cell protrusions which align with local cell velocity¹⁶⁴. Other than active polar terms, one can also set rules to rearrange the local connectivity of vertices to mimic cell division, cell partner switches or cell

extrusion^{14,158}. CPM, vertex and related models have been used to successfully model *in vitro* epithelial systems^{11,325} and epithelial tissue in animal models such as the drosophila¹⁵⁸.

Active matter as a continuum model framework

One emerging class of continuum models used to describe the dynamics of packed, living entities is “active matter”. Here we describe the salient features of such models important for the description of epithelial tissue dynamics, and more details of the models in general can be found in these reviews^{32,326,327}. This class of models is built upon the well-known liquid crystal theories in soft condensed matter physics as living agents usually have an orientable shape and can flow past each other similar to liquid crystal molecules. These models take into consideration generic aspects such as 1) the alignment order of entities with elongated shapes modelled by a nematic order parameter matrix (Figure c), $\mathbf{Q} = 3S(\mathbf{nn} - \mathbf{I}/3)/2$, where \mathbf{n} , the director is a unit vector dictating the local average orientation axis, and $S = \langle \cos 2\theta^{(m)} \rangle$ is the scalar order parameter, with $\theta^{(m)}$ being the angle between each nematic constituent with \mathbf{n} , 2) the broken symmetry distinguishing “head” and “tail” of a nematic entity by a polarity vector, \mathbf{p} (Figure d), 3) passive stress, $\sigma_{ij}^{passive}$ arising from the mesoscopic viscoelasticity of the material, and 4) active stress generation by the individual entities, $\sigma_{ij}^{active} = -\zeta Q_{ij}$. ζ characterizes the strength of the activity, and its sign determine the types of force dipoles that can be generated by cells, i.e. inwards (contractile) or outwards (extensile) force dipoles in the long-axis of the nematic particle³²⁷ (Figure e). The active stress term is the defining feature of a living system and can drive chaotic motion in a system even when it is in the low Reynolds number regime where inertia can be neglected^{328,329}.

In the simplest model of a nematic tissue, mass conservation, momentum conservation and a convection-diffusion equation for the dynamics of the nematic order parameter are used to derive the out-of-equilibrium, hydrodynamic equations. Among the unique features of an active, nematohydrodynamic system include 1) the passive elastic stress arising from the bending, splaying and twisting of the aligned agents, quantified by $\sigma_{ij}^{el} = K(\partial_k Q_{ij})^2/2$, where K is the nematic elastic constant in a single elastic constant approximation and $\partial_k Q_{ij}$ is the spatial gradient of Q_{ij} , 2) the existence of topological defects predominantly of comet and triangle shapes characterized by the lowest possible distortion of the orientation field (Figure f), and 3) unique dynamics for +1/2 defects which have an emergent polar symmetry according to the type of activity as mentioned above³²⁷ (Figure g). It turns out that topological defects in cell alignments, are related to important cellular events such as epithelial cell extrusion and 3D mound formation in neural progenitor cells^{29,242}. On the other hand, polar systems where elongated objects preferentially align with a consistent head or tail direction with their neighbors, or systems with nematically ordered polar objects are more complex, and care must be taken to consider the contribution of \mathbf{p} in the hydrodynamic equations³²⁷. Further, polar systems can only form +1 and -1 defects as the lowest-order defects. Nematic equations have been used to successfully describe a confluent and confined epithelial monolayer or packed single cell types^{29,241,242}, while an expanding monolayer with a free boundary seems to be well described by a polar system²⁵¹. These examples show that *in vitro* epithelial systems are active and complex as they can change their properties i.e. being nematic or polar depending on the geometry and boundary conditions of the system.

Table 1. Summary of surface patterning techniques. The column of Cell types denotes examples of cell types that have been studied using the techniques.

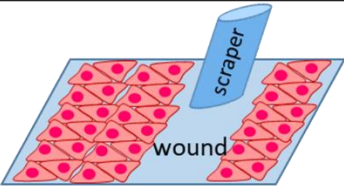
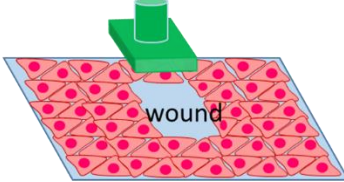
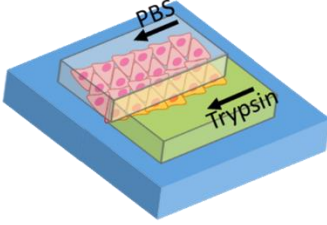
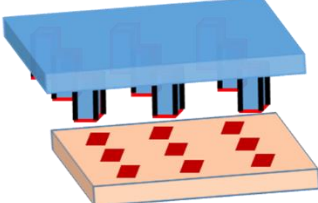
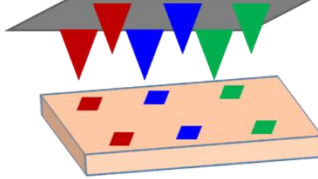
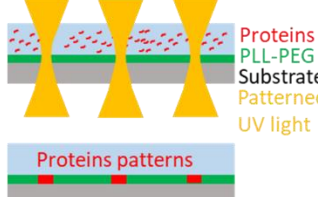
Patterning cell assemblies on planar substrates					
Purposes: Generating free-edges and collective movement to mimic cell migration and invasion					
Techniques	Illustrations	Advantages	Disadvantages	Cell types	Refs
Scratch assay		<ul style="list-style-type: none"> • Low-cost • Convenient 	<ul style="list-style-type: none"> • Poor geometry control • Cause cell death • Require large amount of cells 	<ul style="list-style-type: none"> • Epithelia • Endothelia • Fibroblasts 	46
Model wound assay		<ul style="list-style-type: none"> • Create pristine edge • Defined geometry control • High-throughput 	<ul style="list-style-type: none"> • Involve physical trauma • Advanced fabrication 	<ul style="list-style-type: none"> • Epithelia 	47-51
Microfluidic assay		<ul style="list-style-type: none"> • Damage free denudation • Compatible with chemotaxis tests • High-throughput 	<ul style="list-style-type: none"> • Complicated fabrication 	<ul style="list-style-type: none"> • Epithelia • Endothelia • NIH 3T3 	52,53
Patterning adhesive surfaces					
Purposes: Controlling overall epithelial geometry with adhesive and non-adhesive or switchable surfaces to mimic tissue expansion, homeostasis, and jamming.					
Techniques	Illustrations	Advantages	Disadvantages	Cell types	Refs
Micro-contact printing (μ CP) or micro-stenciling		<ul style="list-style-type: none"> • Good geometry control • High-throughput 	<ul style="list-style-type: none"> • Print dry proteins (μCP) • Difficulties in quantification • Require advanced microfabrication • Difficulties in alignment with multi-protein printing 	<ul style="list-style-type: none"> • Epithelia • Endothelia • Fibroblasts 	43, 54-56
Dip-pen lithography		<ul style="list-style-type: none"> • Nanometer scale resolution 	<ul style="list-style-type: none"> • Sophisticated facility • Serial nature and normally inefficient in producing large and continuous patterns 	<ul style="list-style-type: none"> • Epithelia • Endothelia • Fibroblasts 	57,58
UV patterning		<ul style="list-style-type: none"> • High resolution • Fast reiteration • Potential in creating switchable surface 	<ul style="list-style-type: none"> • Sensitive to surface (hydrophilic) and solution (aqueous) properties 	<ul style="list-style-type: none"> • Epithelia • Endothelia • Fibroblasts 	68-70

Table 2. Techniques for engineering substrate elasticity, viscosity, and topography. The column of Cell types denotes examples of cell types that have been studied using the techniques.

Engineering substrate elasticity and viscosity					
Purposes: Control tissue/material mechanotransduction and mimic physiological viscoelastic properties.					
Techniques	Illustrations	Advantages	Disadvantages	Cell types	Refs
Viscoelastic gel	<p>Elastic gel + Viscous gel → Viscoelastic gel</p>	<ul style="list-style-type: none"> Independently control elasticity and viscosity 	<ul style="list-style-type: none"> Slow loss moduli due to diffusion of the linear chains Limited to PAA (so far) 	<ul style="list-style-type: none"> Fibroblasts Hepatic stellate cells 	83
Modulate rigidity by diffusion	<p>Diffusive area, Droplet of low crosslinker fraction, Increasing rigidity, Droplet of high crosslinker fraction</p>	<ul style="list-style-type: none"> Cheap Convenient 	<ul style="list-style-type: none"> Poor defined stiffness gradient Poor reproducibility Concomitant changes in porosity/surface chemistry 	<ul style="list-style-type: none"> Myoblasts Human stem cells NIH 3T3 Vascular smooth muscle cells 	97-100
Modulate rigidity by temperature	<p>Polymer block, heater, stiffness gradient, Temperature gradient</p>	<ul style="list-style-type: none"> Cheap Convenient 	<ul style="list-style-type: none"> Limited polymer to heat curable Poor reproducibility Concomitant changes in porosity/surface chemistry 	<ul style="list-style-type: none"> Rat mesenchymal stem cells Bone marrow stem cells 	73,74
Modulate rigidity by UV shadowing	<p>UV light, Opaque plate, Mask, Polymer block, Rigidity gradient, Mask withdrawing</p>	<ul style="list-style-type: none"> Enable complex patterning Easy implementation 	<ul style="list-style-type: none"> Poor reproducibility Concomitant changes in porosity/surface chemistry 	<ul style="list-style-type: none"> Epithelia NIH 3T3 	21,75
Compliant soft gel layer	<p>Soft gel layer, Soft, Stiff, Stiff substrate</p>	<ul style="list-style-type: none"> Enable complex patterning Sharp stiffness boundary Uniform porosity/surface chemistry 	<ul style="list-style-type: none"> Complicated fabrication Containing topographic variations 	<ul style="list-style-type: none"> Fibroblasts 	102,103
Pillar arrays	<p>Long pillars, Short pillars, Soft, Stiff, Substrate, Small Ø, large Ø, Soft, Stiff, Substrate</p>	<ul style="list-style-type: none"> Enable complex patterning Sharp stiffness boundary 	<ul style="list-style-type: none"> Advanced fabrication Require sophisticated facilities Discrete surfaces 	<ul style="list-style-type: none"> Epithelia Fibroblasts Endothelia Bovine pulmonary artery smooth muscle cells 	104-106

Engineering substrate topography

Purposes: Control 3D tissue geometry and organization, mimic *in vivo* architectures.

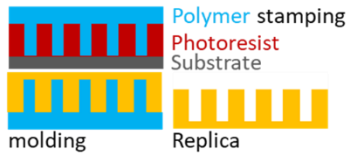
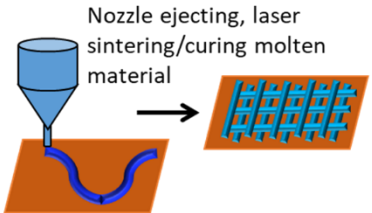
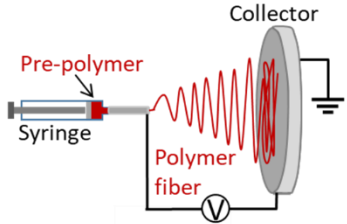
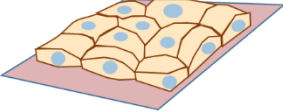
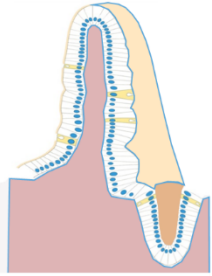
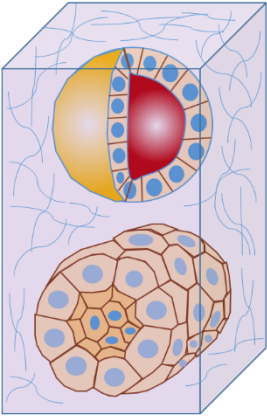
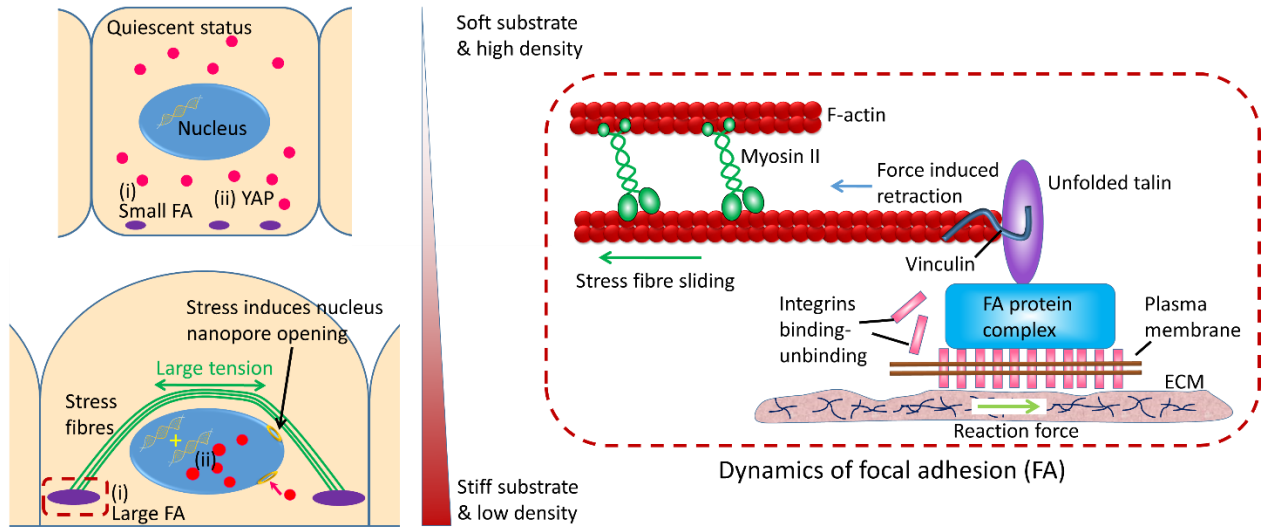
Techniques	Illustrations	Advantages	Disadvantages	Cell types	Refs
Soft lithography	 <p>Polymer stamping Photoresist Substrate molding Replica</p>	<ul style="list-style-type: none"> Versatile and precise patterning Resolution down to tens of nanometer 	<ul style="list-style-type: none"> Sophisticated facility Patterning on curve surface with difficulties 	<ul style="list-style-type: none"> Epithelia Endothelia Fibroblasts 	35
3D printing	 <p>Nozzle ejecting, laser sintering/curing molten material</p>	<ul style="list-style-type: none"> Versatile and precise printing with multiple materials Micrometer resolution 	<ul style="list-style-type: none"> Expansive equipment Time-consuming fabrication Require technical refinement 	<ul style="list-style-type: none"> Epithelial Caco-2 cells 	118
Electro-spinning	 <p>Pre-polymer Syringe Collector Polymer fiber V</p>	<ul style="list-style-type: none"> Produce nano-fibrous surface resembling <i>in vivo</i> substratum Fast and high yield 	<ul style="list-style-type: none"> Require technical refinement 	<ul style="list-style-type: none"> Epithelia Fibroblasts 	119

Table 3. Methods for 2D and 3d culture. The column of Cell types denotes examples of cell types that have been studied using the techniques.

Culture methods	Advantages	Disadvantages	Cell types	Refs
 2D flat substrate	<ul style="list-style-type: none"> • Cheap • Convenient • Versatility for surface modification 	<ul style="list-style-type: none"> • Lack of 3D contact • Absence of gradients of soluble factors in general • Pre-defined apical-basal cell polarity • Cause flat cell morphology 	<ul style="list-style-type: none"> • Epithelia • Endothelia • Stem cells • Fibroblasts 	See Table 1
 Microfabricated substrate with 3D topographic cues	<ul style="list-style-type: none"> • Re-produce topographic aspects of certain physiological conditions 	<ul style="list-style-type: none"> • Lack of soluble gradients in general • Require expensive facilities for fabrication 	<ul style="list-style-type: none"> • Epithelia • Endothelia • Fibroblasts 	31,35,111, 117-119
 3D Hydrogel culture	<ul style="list-style-type: none"> • Cheap • Convenient • Provide 3D contact • Contain soluble gradients • <i>In vivo</i>-like fibrous topography • No pre-defined cell polarity • Rich in bio-ligands 	<ul style="list-style-type: none"> • Naturally extracted hydrogels: batch-to-batch variations, impurities, and undesired immunogenicity • Synthetic hydrogels: bioinert and nondegradable • Both hydrogels: Intertwined parameters 	<ul style="list-style-type: none"> • Epithelia • Endothelia • Fibroblasts 	121-127

a

- i. Mechanical stress induces the enlargement of FAs.
- ii. Under high stress, YAP rapidly relocalizes to nucleus to activate gene transcription.



b

- i. High tension at AJs causes β -catenin to displace into cytoplasm and later nucleus.
- ii. Stress in membrane induce opening of Piezo ion channel, triggering Ca^{2+} -mediated pathway.

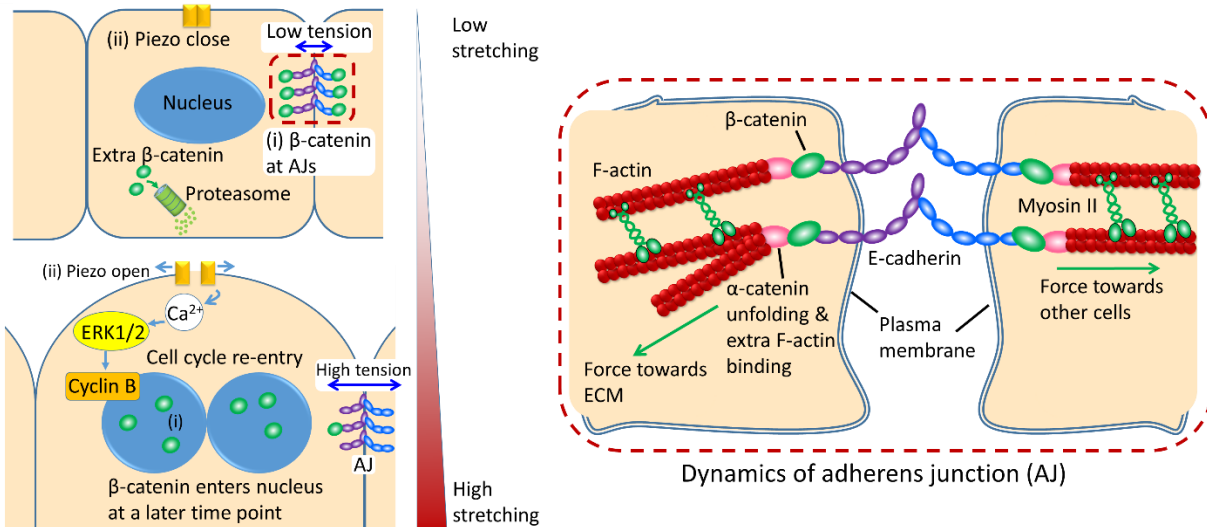


Figure 1. Mechanosensitive molecular networks and signalling. **a)** Distinct molecular responses to cell-substrate interaction, compared and illustrated between epithelia with low and high tensile stress/cell density. (i) Cells in a monolayer spread more in a low density tissue and have stronger cell-substrate interaction. This leads to larger tension within stress fibers that promotes active FA growth to sustain this high stress. At high cell density, cell-cell junctions become more mature with a concomitant decrease in cell-substrate traction forces and smaller FAs²⁵². (ii) At low density, the transcription factor YAP is activated within the nucleus to induce gene transcription, while in crowded tissues, the YAP is de-activated and delocalized from the nucleus, leading to more cell death^{202,207}. One pathway that can lead to facilitate YAP translocation into the nucleus at low cell density is the compression of the nucleus by strong apical stress fibers leading to the opening of nuclear-pores²⁰⁸. All these mechanotransductive pathways allow the monolayer to sense the mechanical environment which includes cell density and similarly substrate

stiffness and regulate tissue homeostasis correspondingly. Inset: The building of a stable FA complex for cell-substrate adhesion. Acto-myosin contractile forces pull on the FA at a constant speed and the rate of force increase in the complex increases proportionally with the ECM stiffness. The binding-unbinding rates of the transmembrane protein, integrin, that connects the cells to the substrate needs to match the force loading rate in the complex to ensure the FA does not destabilize and detach. Talin serves as a force buffer and mechanosensor in the FA. Its unfolding at ~ 10 pN at the normal rate of force loading in cells lead to vinculin binding to recruit more actin fibers, thus reinforcing the FA²²¹. **b)** Molecular mechanosensing response to mechanical stretching. (i) When the monolayer is mechanically stretched, leading to lower cell density and higher tension at AJs, the β -catenin proteins, which are usually localized at the intercellular part of mature AJs as adaptor proteins at high density tissues, are displaced from the junctions and can shuttle into the nucleus to initiate cell division. (ii) At high density and cell crowding conditions, mechanosensitive ion channel, Piezo is possibly activated and develops into aggregates in the cytoplasm and thus induces live cell extrusion^{13,150}. At low cell density, the increase in cell division events is related to Piezo activities as well, and could be due to a redistribution of the ions from the outer plasma membrane into membranes within the cell¹⁵⁰. Inset: Dynamics of adherens junction. AJs are subjected to forces transmitted from cell-substrate and cell-cell interactions, mediated mainly by actomyosin activities. Increasing tension at AJs leads to α -catenin unfolding and subsequently the recruitment of vinculin and extra F-actin to stabilize the AJ structure²³³. Also, traction forces are able to propagate deep into the tissue among cells coupled via AJs.

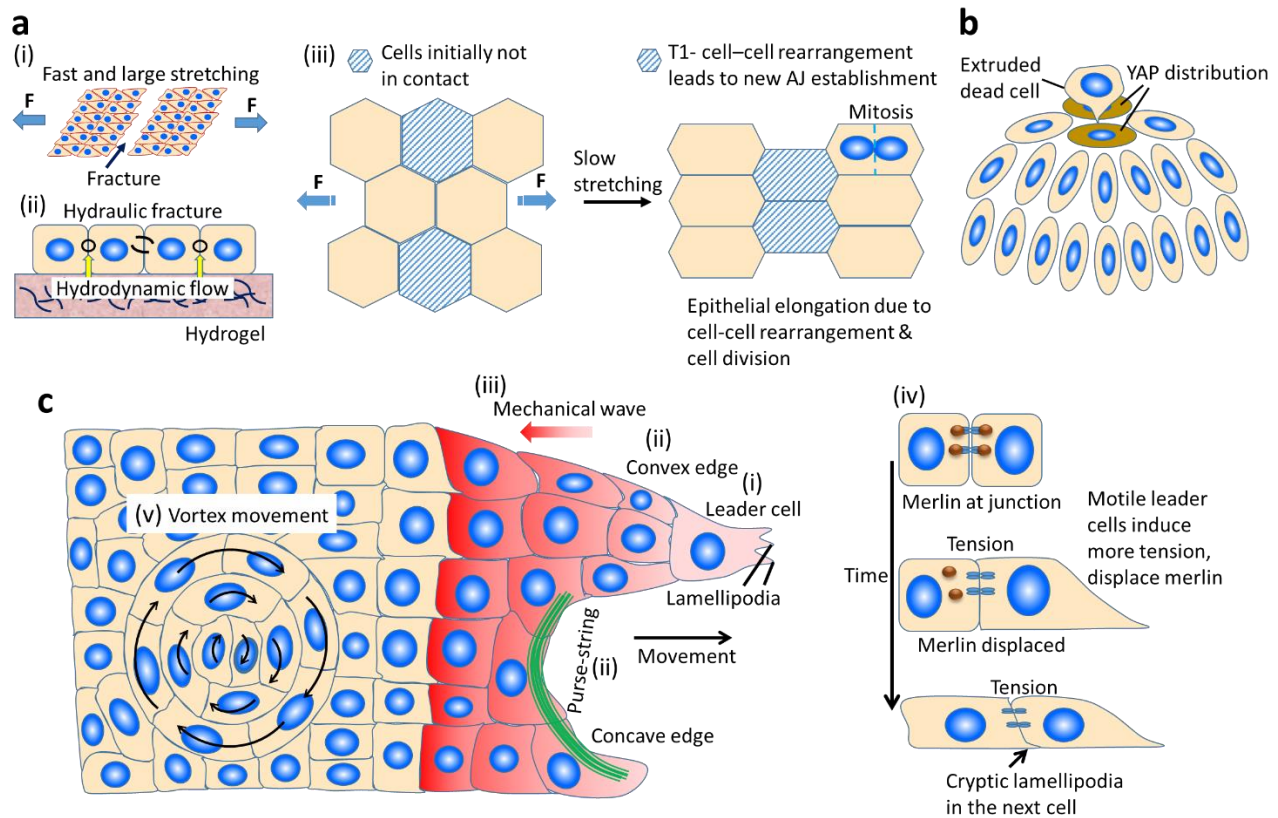


Figure 2. Tissue as an active matter. **a)** Monolayer response to external mechanical stretch. (i) Fast and huge stretching leads to monolayer tearing preferentially initiated at cell-cell junctions¹⁸⁰. (ii) The stretch-relaxation loading of hydrogels lead to water influx and swelling, then water expulsion. When coupled to a monolayer from below, this hydrogel-induced hydrodynamic generates cracks in the monolayer at the cell-cell junctions²³⁷. (iii) Under slow stretching, cell-cell rearrangement accompanied by cell-cell junction remodeling¹⁷⁷, and induced cell division^{149,240} can lead to stress relaxation and elongation of the tissue in the direction of stretch. **b)** +1/2 or comet shaped cell misalignment patterns in the epithelial monolayer leads to high compressive stress due to the elastic bending of a group of cells, triggering caspase-3 activation, cell death and extrusion²⁹. Similarly, +1/2 defects in neural progenitor cell collectives lead to 3D mound formation²⁴². **c)** Mechanical force transmission within a monolayer during epithelial expansion. (i) A leader cell forms at the tissue front with large lamellipodia and pulls along behind it a multicellular finger²⁴⁵. (ii) The lamellipodia preferentially emerges at a convex edge, while concave edges form transcellular actin cables⁴⁵. Both actin-mediated structures drive epithelial expansion. (iii) As the cells at the front moves forward, a strain wave propagates backward into the tissue, progressively stretching the cells behind and thus mechanically activating these cells to move forward too¹⁰. (iv) When cells are stretched from the front, this displaces their merlin protein distribution at the cell-cell junction which originally inhibits Rac activity³⁷. This leads to cryptic lamellipodia formation from the cell at the back to follow the cell movement in front of it. (v) Tissue dynamics is typically chaotic, and there can be vortex movement instead of purely straightforward motion within the monolayer during epithelial expansion¹⁸².

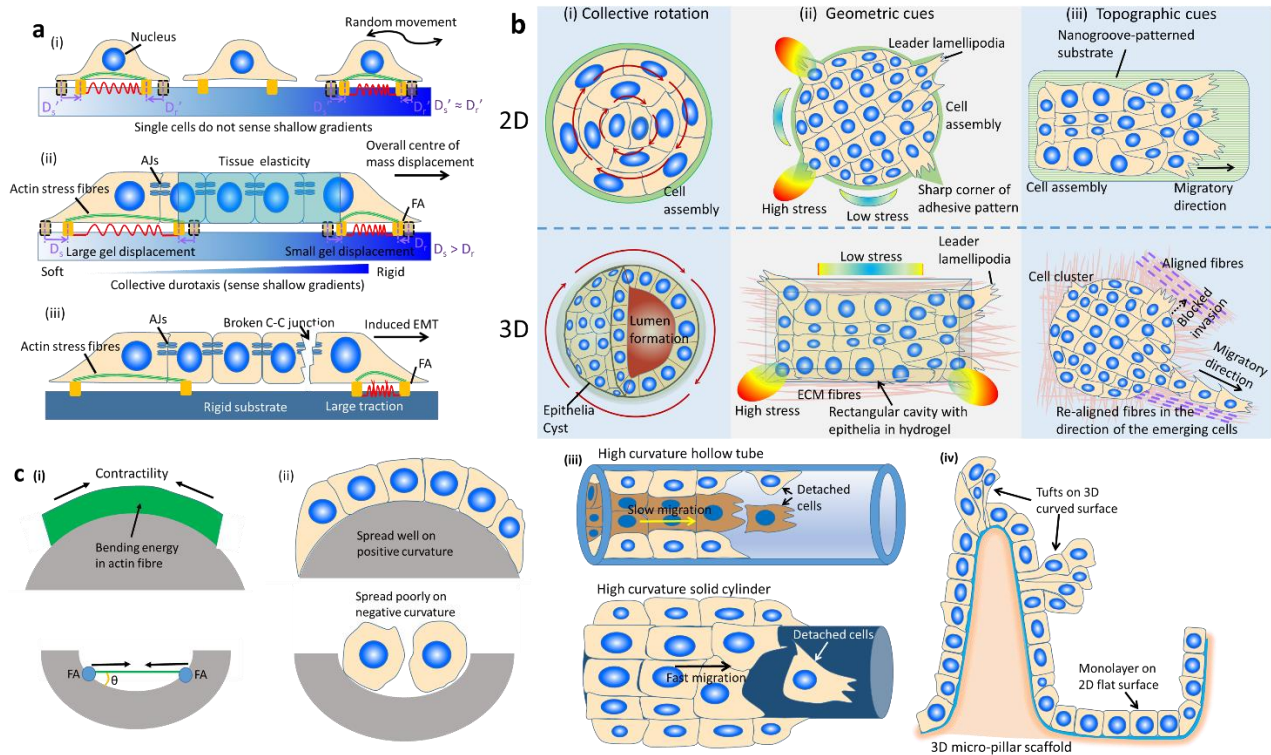


Figure 3. Active tissue response to its mechanical environment. a) Response to substrate stiffness. (i) Cell-cell junction connects multiple cells to form a monolayer which acts like a ‘giant cell’. The connected monolayer can sense shallow stiffness gradients, whilst a monolayer with weakened junctions such as α -catenin knocked down cells cannot²¹. (ii) In collective durotaxis, both edges of an expanding monolayer (one on the softer side, while the other on the stiffer side) exert the same traction forces. However, the softer substrate displaces (D_x and D_x') more and thus the overall centre of mass of the monolayer moves in the direction of the stiffer regions²¹. (iii) On stiffer substrates, cells exert larger traction forces which gets transmitted within the monolayer through cell-cell junctions, which could destabilize the junctions. It is known that the EMT transition can be triggered on stiff substrates, where cells switch from E- to N-cadherin at their junctions. N-cadherin promotes cell scattering from the collective, unlike E-cadherin which allows cells to stick to each other. **b)** 2D vs 3D responses. (i) When confined in a circular adhesive pattern, epithelial monolayer can display orderly collective cell movement, such as coherent rotation. Similar rotational motion in 3D epithelia cysts embedded in hydrogel have been observed. Further, as cells are presented with the ECM proteins from all sides in a 3D gel, cells can polarize and form lumen within the tissue²⁸⁴. (ii) Leader cells with large lamellipodia can emerge at the corners of a 3D, rectangular-shaped tissue within a gel²⁸⁵, similar to tissue on 2D patterns with sharp corners²⁴⁸. This phenomenon is related to the localization of higher mechanical stress, originating from active tissue stress, at the edges due to the specific geometry. (iii) Surface topographic cues like nanogrooves on 2D can guide epithelial expansion. Similarly, leader cells can realign collagen fibers in 3D¹⁶⁶ to create tracks for follower cells to move in the same direction. However, cell migration can be blocked by tangentially aligned fibres as observed in CAF-assisted cancer invasion²⁷. **c)** Response to out-of-plane curvatures. (i) Contractile stress-induced energy balances bending energy of the stress fiber to promote an optimal alignment of stress fiber with the surface curvature on surfaces with positive curvature³⁰⁵. On surfaces with negative curvature, the FA is being pulled at an angle with the local underlying substrate by the stress fiber, and the increased loading

angle enhances FA detachment from the substrate³⁰⁹. (ii) At the tissue level, monolayers are known to spread on surfaces with positive curvature, while cells do not spread well on those with negative curvature, thus inhibiting monolayer formation. (iii) Tubular epithelial structures move slowly in highly curved inner surfaces of a tube¹¹⁰ but moves fast on the outer surface of a cylinder¹⁰⁹. In both scenarios the cells at the front tend to detach from the collective, reminiscent of EMT. (iv) AJ-compromised epithelia can still form a normal monolayer on flat substrates but not on villi-like structures with positive curvatures, they form tufts instead³¹.

References

1. Alberts, B. *Molecular biology of the cell*. (Garland Science, New York, 2008).
2. Sakar, M. S. *et al.* Cellular forces and matrix assembly coordinate fibrous tissue repair. *Nat. Commun.* **7**, 11036 (2016).
3. Cetera, M. *et al.* Epithelial rotation promotes the global alignment of contractile actin bundles during *Drosophila* egg chamber elongation. *Nat. Commun.* **5**, 5511 (2014).
4. Puliafito, A. *et al.* Collective and single cell behavior in epithelial contact inhibition. *Proc. Natl. Acad. Sci. USA* **109**, 739–744 (2012).
5. Giampieri, S. *et al.* Localized and reversible TGF β signalling switches breast cancer cells from cohesive to single cell motility. *Nat. Cell Biol.* **11**, 1287–1296 (2009).
6. Park, J.-A. *et al.* Unjamming and cell shape in the asthmatic airway epithelium. *Nat. Mater.* **14**, 1040–1048 (2015).
7. Collinet, C., Rauzi, M., Lenne, P.-F. & Lecuit, T. Local and tissue-scale forces drive oriented junction growth during tissue extension. *Nat. Cell Biol.* **17**, 1247–1258 (2015).
8. Ladoux, B. & Mège, R.-M. Mechanobiology of collective cell behaviours. *Nat. Rev. Mol. Cell Biol.* **18**, 743 (2017).
9. Balaji, R. *et al.* Calcium spikes, waves and oscillations in a large, patterned epithelial tissue. *Sci. Rep.* **7**, 42786 (2017).
10. Serra-Picamal, X. *et al.* Mechanical waves during tissue expansion. *Nat. Phys.* **8**, 628–634 (2012).
11. Vedula, S. R. K. *et al.* Emerging modes of collective cell migration induced by geometrical constraints. *Proc. Natl. Acad. Sci. USA* **109**, 12974–12979 (2012).
12. Gomez, G. A., McLachlan, R. W. & Yap, A. S. Productive tension: force-sensing and homeostasis of cell–cell junctions. *Trends Cell Biol.* **21**, 499–505 (2011).
13. Eisenhoffer, G. T. *et al.* Crowding induces live cell extrusion to maintain homeostatic cell numbers in epithelia. *Nature* **484**, 546 (2012).
14. Marinari, E. *et al.* Live-cell delamination counterbalances epithelial growth to limit tissue overcrowding. *Nature* **484**, 542 (2012).
15. Halbleib, J. M. & Nelson, W. J. Cadherins in development: cell adhesion, sorting, and tissue morphogenesis. *Genes Dev.* **20**, 3199–3214 (2006).
16. Maruthamuthu, V., Sabass, B., Schwarz, U. S. & Gardel, M. L. Cell-ECM traction force modulates

- endogenous tension at cell–cell contacts. *Proc. Natl. Acad. Sci. USA* **108**, 4708–4713 (2011).
17. Mège, R. M. & Ishiyama, N. Integration of Cadherin Adhesion and Cytoskeleton at Adherens Junctions. *Cold Spring Harb. Perspect. Biol.* (2017).
 18. Mizuno, D., Tardin, C., Schmidt, C. F. & MacKintosh, F. C. Nonequilibrium mechanics of active cytoskeletal networks. *Science (80-.)*. **315**, 370–373 (2007).
 19. Gupta, M. *et al.* Adaptive rheology and ordering of cell cytoskeleton govern matrix rigidity sensing. *Nat. Commun.* **6**, 7525 (2015).
 20. Barriga, E. H., Franze, K., Charras, G. & Mayor, R. Tissue stiffening coordinates morphogenesis by triggering collective cell migration in vivo. *Nature* **554**, 523 (2018).
 21. Sunyer, R. *et al.* Collective cell durotaxis emerges from long-range intercellular force transmission. *Science (80-.)*. **353**, 1157–1161 (2016).
 22. Haigo, S. L. & Bilder, D. Global Tissue Revolutions in a Morphogenetic Movement Controlling Elongation. *Science (80-.)*. **331**, 1071–1074 (2011).
 23. Shields, M. A., Dangi-Garimella, S., Redig, A. J. & Munshi, H. G. Biochemical role of the collagen-rich tumour microenvironment in pancreatic cancer progression. *Biochem. J.* **441**, 541 LP-552 (2012).
 24. Glentis, A. *et al.* Cancer-associated fibroblasts induce metalloprotease-independent cancer cell invasion of the basement membrane. *Nat. Commun.* **8**, 924 (2017).
 25. Grossman, M. *et al.* Tumor Cell Invasion Can Be Blocked by Modulators of Collagen Fibril Alignment That Control Assembly of the Extracellular Matrix. *Cancer Res.* **76**, 4249 LP-4258 (2016).
 26. Provenzano, P. P. *et al.* Collagen reorganization at the tumor-stromal interface facilitates local invasion. *BMC Med.* **4**, 38 (2006).
 27. Erdogan, B. *et al.* Cancer-associated fibroblasts promote directional cancer cell migration by aligning fibronectin. *J Cell Biol* jcb. 201704053 (2017).
 28. Ruprecht, V. *et al.* How cells respond to environmental cues – insights from bio-functionalized substrates. *J. Cell Sci.* **130**, 51 LP-61 (2017).
 29. Saw, T. B. *et al.* Topological defects in epithelia govern cell death and extrusion. *Nature* **544**, 212 (2017).
 30. Nelson, C. M. *et al.* Emergent patterns of growth controlled by multicellular form and mechanics. *Proc. Natl. Acad. Sci. USA* **102**, 11594–11599 (2005).
 31. Salomon, J. *et al.* Contractile forces at tricellular contacts modulate epithelial organization and monolayer integrity. *Nat. Commun.* **8**, 13998 (2017).
 32. Prost, J., Jülicher, F. & Joanny, J. F. Active gel physics. *Nat. Phys.* **11**, 111–117 (2015).
 33. Huang, G. *et al.* Functional and Biomimetic Materials for Engineering of the Three-Dimensional Cell Microenvironment. *Chem. Rev.* **117**, 12764–12850 (2017).
 34. Rosales, A. M. & Anseth, K. S. The design of reversible hydrogels to capture extracellular matrix dynamics. *Nat. Rev. Mater.* **1**, 15012 (2016).
 35. Xia, Y. N. & Whitesides, G. M. Soft lithography. *Angew. Chemie-International Ed.* **37**, 550–575

(1998).

36. Vedula, S. R. K. *et al.* Mechanics of epithelial closure over non-adherent environments. *Nat. Commun.* **6**, 6111 (2015).
37. Das, T. *et al.* A molecular mechanotransduction pathway regulates collective migration of epithelial cells. *Nat. Cell Biol.* **17**, 276–287 (2015).
38. Segerer, F. J., Thüroff, F., Piera Alberola, A., Frey, E. & Rädler, J. O. Emergence and persistence of collective cell migration on small circular micropatterns. *Phys. Rev. Lett.* **114**, 228102 (2015).
39. Wong, I. Y. *et al.* Collective and individual migration following the epithelial–mesenchymal transition. *Nat. Mater.* **13**, 1063–1071 (2014).
40. Karuri, N. W. *et al.* Biological length scale topography enhances cell-substratum adhesion of human corneal epithelial cells. *J. Cell Sci.* **117**, 3153 LP-3164 (2004).
41. Shao, Y. & Fu, J. Integrated Micro/Nanoengineered Functional Biomaterials for Cell Mechanics and Mechanobiology: A Materials Perspective. *Adv. Mater.* **26**, 1494–1533 (2013).
42. Théry, M. Micropatterning as a tool to decipher cell morphogenesis and functions. *J. Cell Sci.* **123**, 4201 LP-4213 (2010).
43. Alom Ruiz, S. & Chen, C. S. Microcontact printing: A tool to pattern. *Soft Matter* **3**, 168–177 (2007).
44. Curtis, A. S., Forrester, J. V, McInnes, C. & Lawrie, F. Adhesion of cells to polystyrene surfaces. *J. Cell Biol.* **97**, 1500 LP-1506 (1983).
45. Ravasio, A. *et al.* Regulation of epithelial cell organization by tuning cell-substrate adhesion. *Integr. Biol.* **7**, 1228–1241 (2015).
46. Liang, C.-C., Park, A. Y. & Guan, J.-L. In vitro scratch assay: a convenient and inexpensive method for analysis of cell migration in vitro. *Nat. Protoc.* **2**, 329 (2007).
47. Djordje L. Nikolić, Alistair N. Boettiger, Dafna Bar-Sagi, Jeffrey D. Carbeck, and S. Y. S. Role of boundary conditions in an experimental model of epithelial wound healing. *Am. J. Physiol. Physiol.* **291**, C68–C75 (2006).
48. Fong, E., Tzllil, S. & Tirrell, D. A. Boundary crossing in epithelial wound healing. *Proc. Natl. Acad. Sci. USA* **107**, 19302–19307 (2010).
49. Poujade, M. *et al.* Collective migration of an epithelial monolayer in response to a model wound. *Proc. Natl. Acad. Sci. USA* **104**, 15988–15993 (2007).
50. Ravasio, A. *et al.* Gap geometry dictates epithelial closure efficiency. *Nat. Commun.* **6**, 7683 (2015).
51. Anon, E. *et al.* Cell crawling mediates collective cell migration to close undamaged epithelial gaps. *Proc. Natl. Acad. Sci. USA* **109**, 10891–10896 (2012).
52. Murrell, M., Kamm, R. & Matsudaira, P. Tension, Free Space, and Cell Damage in a Microfluidic Wound Healing Assay. *PLoS One* **6**, e24283 (2011).
53. Nie, F.-Q. *et al.* On-chip cell migration assay using microfluidic channels. *Biomaterials* **28**, 4017–4022 (2007).
54. Doxzen, K. *et al.* Guidance of collective cell migration by substrate geometry. *Integr. Biol.* **5**,

1026–1035 (2013).

55. Desai, R. A., Rodriguez, N. M. & Chen, C. S. in *Micropatterning in Cell Biology Part A* (eds. Piel, M. & Théry, M. B. T.-M. in C. B.) **119**, 3–16 (Academic Press, 2014).
56. Masters, T. *et al.* Easy Fabrication of Thin Membranes with Through Holes. Application to Protein Patterning. *PLoS One* **7**, e44261 (2012).
57. Piner, R. D., Zhu, J., Xu, F., Hong, S. & Mirkin, C. A. ‘Dip-Pen’ Nanolithography. *Science* (80-.). **283**, 661–663 (1999).
58. Huo, F. *et al.* Polymer Pen Lithography. *Science* (80-.). **321**, 1658–1660 (2008).
59. Tse, J. R. & Engler, A. J. Preparation of Hydrogel Substrates with Tunable Mechanical Properties. *Curr. Protoc. Cell Biol.* **47**, 10.16.1-10.16.16 (2010).
60. Wenqian, F. *et al.* Surface Patterning via Thiol-Yne Click Chemistry: An Extremely Fast and Versatile Approach to Superhydrophilic-Superhydrophobic Micropatterns. *Adv. Mater. Interfaces* **1**, 1400269 (2014).
61. Pelham, R. J. & Wang, Y. Cell locomotion and focal adhesions are regulated by substrate flexibility. *Proc. Natl. Acad. Sci. USA* **94**, 13661–13665 (1997).
62. Grevesse, T., Versaevel, M., Circelli, G., Desprez, S. & Gabriele, S. A simple route to functionalize polyacrylamide hydrogels for the independent tuning of mechanotransduction cues. *Lab Chip* **13**, 777–780 (2013).
63. Cavalcanti-Adam, E. A. *et al.* Cell Spreading and Focal Adhesion Dynamics Are Regulated by Spacing of Integrin Ligands. *Biophys. J.* **92**, 2964–2974 (2007).
64. Arnold, M. *et al.* Activation of Integrin Function by Nanopatterned Adhesive Interfaces. *ChemPhysChem* **5**, 383–388 (2004).
65. Oria, R. *et al.* Force loading explains spatial sensing of ligands by cells. *Nature* **552**, 219 (2017).
66. Cohen, D. J., Gloerich, M. & Nelson, W. J. Epithelial self-healing is recapitulated by a 3D biomimetic E-cadherin junction. *Proc. Natl. Acad. Sci. USA* **113**, 14698–14703 (2016).
67. Li, Q. *et al.* Extracellular matrix scaffolding guides lumen elongation by inducing anisotropic intercellular mechanical tension. *Nat. Cell Biol.* **18**, 311–318 (2016).
68. Azioune, A., Storch, M., Bornens, M., Théry, M. & Piel, M. Simple and rapid process for single cell micro-patterning. *Lab Chip* **9**, 1640–1642 (2009).
69. Pasche, S., De Paul, S. M., Vörös, J., Spencer, N. D. & Textor, M. Poly(l-lysine)-graft-poly(ethylene glycol) Assembled Monolayers on Niobium Oxide Surfaces: A Quantitative Study of the Influence of Polymer Interfacial Architecture on Resistance to Protein Adsorption by ToF-SIMS and in Situ OWLS. *Langmuir* **19**, 9216–9225 (2003).
70. Strale, P.-O. *et al.* Multiprotein Printing by Light-Induced Molecular Adsorption. *Adv. Mater.* **28**, 2024–2029 (2016).
71. Rolli, C. G. *et al.* Switchable adhesive substrates: Revealing geometry dependence in collective cell behavior. *Biomaterials* **33**, 2409–2418 (2012).
72. Kim, S. N. *et al.* ECM stiffness regulates glial migration in Drosophila and mammalian glioma models. *Development* **141**, 3233 LP-3242 (2014).

73. Wang, P.-Y., Tsai, W.-B. & Voelcker, N. H. Screening of rat mesenchymal stem cell behaviour on polydimethylsiloxane stiffness gradients. *Acta Biomater.* **8**, 519–530 (2012).
74. Kim, T. H. *et al.* Creating stiffness gradient polyvinyl alcohol hydrogel using a simple gradual freezing–thawing method to investigate stem cell differentiation behaviors. *Biomaterials* **40**, 51–60 (2015).
75. Sunyer, R., Jin, A. J., Nossal, R. & Sackett, D. L. Fabrication of Hydrogels with Steep Stiffness Gradients for Studying Cell Mechanical Response. *PLoS One* **7**, e46107 (2012).
76. Vincent, L. G., Choi, Y. S., Alonso-Latorre, B., del Álamo, J. C. & Engler, A. J. Mesenchymal stem cell durotaxis depends on substrate stiffness gradient strength. *Biotechnol. J.* **8**, 472–484 (2013).
77. J., B. S. & S., A. K. Hydrogel properties influence ECM production by chondrocytes photoencapsulated in poly(ethylene glycol) hydrogels. *J. Biomed. Mater. Res.* **59**, 63–72 (2001).
78. Marklein, R. A. & Burdick, J. A. Spatially controlled hydrogel mechanics to modulate stem cell interactions. *Soft Matter* **6**, 136–143 (2010).
79. Willits, R. K. & Skornia, S. L. Effect of collagen gel stiffness on neurite extension. *J. Biomater. Sci. Polym. Ed.* **15**, 1521–1531 (2004).
80. Murrell, M., Kamm, R. & Matsudaira, P. Substrate Viscosity Enhances Correlation in Epithelial Sheet Movement. *Biophys. J.* **101**, 297–306 (2011).
81. Trappmann, B. *et al.* Extracellular-matrix tethering regulates stem-cell fate. *Nat. Mater.* **11**, 642 (2012).
82. Zheng, J. Y. *et al.* Epithelial Monolayers Coalesce on a Viscoelastic Substrate through Redistribution of Vinculin. *Biophys. J.* **113**, 1585–1598 (2017).
83. Charrier, E. E., Pogoda, K., Wells, R. G. & Janmey, P. A. Control of cell morphology and differentiation by substrates with independently tunable elasticity and viscous dissipation. *Nat. Commun.* **9**, 449 (2018).
84. Rao, R. R., Peterson, A. W., Ceccarelli, J., Putnam, A. J. & Stegeman, J. P. Matrix composition regulates three-dimensional network formation by endothelial cells and mesenchymal stem cells in collagen/fibrin materials. *Angiogenesis* **15**, 253–264 (2012).
85. Zaman, M. H. *et al.* Migration of tumor cells in 3D matrices is governed by matrix stiffness along with cell-matrix adhesion and proteolysis. *Proc. Natl. Acad. Sci.* **103**, 10889 LP-10894 (2006).
86. Roeder, B. A., Kokini, K., Sturgis, J. E., Robinson, J. P. & Voytik-Harbin, S. L. Tensile Mechanical Properties of Three-Dimensional Type I Collagen Extracellular Matrices With Varied Microstructure. *J. Biomech. Eng.* **124**, 214–222 (2002).
87. McDaniel, D. P. *et al.* The Stiffness of Collagen Fibrils Influences Vascular Smooth Muscle Cell Phenotype. *Biophys. J.* **92**, 1759–1769 (2007).
88. Francis-Sedlak, M. E. *et al.* Characterization of type I collagen gels modified by glycation. *Biomaterials* **30**, 1851–1856 (2009).
89. Mason, B. N., Starchenko, A., Williams, R. M., Bonassar, L. J. & Reinhart-King, C. A. Tuning three-dimensional collagen matrix stiffness independently of collagen concentration modulates endothelial cell behavior. *Acta Biomater.* **9**, 4635–4644 (2013).

90. Thomas, M. C., Baynes, J. W. & Cooper, S. R. T. and M. E. The Role of AGEs and AGE Inhibitors in Diabetic Cardiovascular Disease. *Current Drug Targets* **6**, 453–474 (2005).
91. Taguchi, A. *et al.* Blockade of RAGE–amphoterin signalling suppresses tumour growth and metastases. *Nature* **405**, 354 (2000).
92. Licup, A. J. *et al.* Stress controls the mechanics of collagen networks. *Proc. Natl. Acad. Sci.* **112**, 9573 LP-9578 (2015).
93. Nam, S., Hu, K. H., Butte, M. J. & Chaudhuri, O. Strain-enhanced stress relaxation impacts nonlinear elasticity in collagen gels. *Proc. Natl. Acad. Sci.* **113**, 5492–5497 (2016).
94. Kim, J. *et al.* Stress-induced plasticity of dynamic collagen networks. *Nat. Commun.* **8**, 842 (2017).
95. Ban, E. *et al.* Mechanisms of Plastic Deformation in Collagen Networks Induced by Cellular Forces. *Biophys. J.* **114**, 450–461 (2018).
96. de Wild, M., Pomp, W. & Koenderink, G. H. Thermal Memory in Self-Assembled Collagen Fibril Networks. *Biophys. J.* **105**, 200–210 (2013).
97. Lo, C. T., Throckmorton, D. J., Singh, A. K. & Herr, A. E. Photopolymerized diffusion-defined polyacrylamide gradient gels for on-chip protein sizing. *Lab Chip* **8**, 1273–1279 (2008).
98. Hadden, W. J. *et al.* Stem cell migration and mechanotransduction on linear stiffness gradient hydrogels. *Proc. Natl. Acad. Sci. USA* **114**, 5647–5652 (2017).
99. Lo, C.-M., Wang, H.-B., Dembo, M. & Wang, Y. Cell Movement Is Guided by the Rigidity of the Substrate. *Biophys. J.* **79**, 144–152 (2000).
100. Hartman, C. D., Isenberg, B. C., Chua, S. G. & Wong, J. Y. Vascular smooth muscle cell durotaxis depends on extracellular matrix composition. *Proc. Natl. Acad. Sci. USA* **113**, 11190–11195 (2016).
101. Stephanie, N., N., H. H. & L., W. J. PEGDA hydrogels with patterned elasticity: Novel tools for the study of cell response to substrate rigidity. *Biotechnol. Bioeng.* **105**, 636–644 (2009).
102. Kuo, C. R., Xian, J., Brenton, J. D., Franze, K. & Sivaniah, E. Complex Stiffness Gradient Substrates for Studying Mechanotactic Cell Migration. *Adv. Mater.* **24**, 6059–6064 (2012).
103. Wong, S., Guo, W.-H. & Wang, Y.-L. Fibroblasts probe substrate rigidity with filopodia extensions before occupying an area. *Proc. Natl. Acad. Sci. USA* **111**, 17176–17181 (2014).
104. Tan, J. L. *et al.* Cells lying on a bed of microneedles: An approach to isolate mechanical force. *Proc. Natl. Acad. Sci. USA* **100**, 1484–1489 (2003).
105. Saez, A., Ghibaudo, M., Buguin, A., Silberzan, P. & Ladoux, B. Rigidity-driven growth and migration of epithelial cells on microstructured anisotropic substrates. *Proc. Natl. Acad. Sci. USA* **104**, 8281–8286 (2007).
106. Trichet, L. *et al.* Evidence of a large-scale mechanosensing mechanism for cellular adaptation to substrate stiffness. *Proc. Natl. Acad. Sci. USA* **109**, 6933–6938 (2012).
107. Tong, M. H., Huang, N., Ngan, A. H. W., Du, Y. & Chan, B. P. Preferential sensing and response to microenvironment stiffness of human dermal fibroblast cultured on protein micropatterns fabricated by 3D multiphoton biofabrication. *Sci. Rep.* **7**, 12402 (2017).
108. Lipton, J. I. & Lipson, H. 3D Printing Variable Stiffness Foams Using Viscous Thread Instability. *Sci. Rep.* **6**, 29996 (2016).

109. Yevick, H. G., Duclos, G., Bonnet, I. & Silberzan, P. Architecture and migration of an epithelium on a cylindrical wire. *Proc. Natl. Acad. Sci. USA* **112**, 5944–5949 (2015).
110. Xi, W., Sonam, S., Saw, T. B., Ladoux, B. & Lim, C. T. Emergent patterns of collective cell migration under tubular confinement. *Nat. Commun.* **8**, 1517 (2017).
111. Wang, Y. *et al.* A microengineered collagen scaffold for generating a polarized crypt-villus architecture of human small intestinal epithelium. *Biomaterials* **128**, 44–55 (2017).
112. Teixeira, A. I., Abrams, G. A., Bertics, P. J., Murphy, C. J. & Nealey, P. F. Epithelial contact guidance on well-defined micro- and nanostructured substrates. *J. Cell Sci.* **116**, 1881–1892 (2003).
113. Clark, P., Connolly, P., Curtis, A. S., Dow, J. A. & Wilkinson, C. D. Topographical control of cell behaviour: II. Multiple grooved substrata. *Development* **108**, 635 LP-644 (1990).
114. Xia, Y. *et al.* Complex Optical Surfaces Formed by Replica Molding Against Elastomeric Masters. *Science (80-.)*. **273**, 347–349 (1996).
115. Qin, D., Xia, Y. & Whitesides, G. M. Soft lithography for micro- and nanoscale patterning. *Nat. Protoc.* **5**, 491 (2010).
116. Sung, J. H., Yu, J., Luo, D., Shuler, M. L. & March, J. C. Microscale 3-D hydrogel scaffold for biomimetic gastrointestinal (GI) tract model. *Lab Chip* **11**, 389–392 (2011).
117. Jiajie, Y., Songming, P., Dan, L. & C., M. J. In vitro 3D human small intestinal villous model for drug permeability determination. *Biotechnol. Bioeng.* **109**, 2173–2178 (2012).
118. Costello, C. M. *et al.* Microscale Bioreactors for in situ characterization of GI epithelial cell physiology. *Sci. Rep.* **7**, 12515 (2017).
119. Schindler, M. *et al.* A synthetic nanofibrillar matrix promotes in vivo-like organization and morphogenesis for cells in culture. *Biomaterials* **26**, 5624–5631 (2005).
120. Saha, S. *et al.* Electrospun Fibrous Scaffolds Promote Breast Cancer Cell Alignment and Epithelial–Mesenchymal Transition. *Langmuir* **28**, 2028–2034 (2012).
121. Barcellos-Hoff, M. H., Aggeler, J., Ram, T. G. & Bissell, M. J. Functional differentiation and alveolar morphogenesis of primary mammary cultures on reconstituted basement membrane. *Development* **105**, 223 LP-235 (1989).
122. Nelson, C. M., Inman, J. L. & Bissell, M. J. Three-dimensional lithographically defined organotypic tissue arrays for quantitative analysis of morphogenesis and neoplastic progression. *Nat. Protoc.* **3**, 674 (2008).
123. Lynn, A. K., Yannas, I. V. & Bonfield, W. Antigenicity and immunogenicity of collagen. *J. Biomed. Mater. Res. Part B Appl. Biomater.* **71B**, 343–354 (2004).
124. Lim, K. S., Martens, P. & Poole-Warren, L. in *Functional Hydrogels as Biomaterials* (eds. Li, J., Osada, Y. & Cooper-White, J.) 1–29 (Springer Berlin Heidelberg, 2018). doi:10.1007/978-3-662-57511-6_1
125. Gjorevski, N. *et al.* Designer matrices for intestinal stem cell and organoid culture. *Nature* **539**, 560–564 (2016).
126. Sato, T. & Clevers, H. Growing Self-Organizing Mini-Guts from a Single Intestinal Stem Cell: Mechanism and Applications. *Science (80-.)*. **340**, 1190–1194 (2013).

127. Lee, G. Y., Kenny, P. A., Lee, E. H. & Bissell, M. J. Three-dimensional culture models of normal and malignant breast epithelial cells. *Nat. Methods* **4**, 359 (2007).
128. Nelson, C. M., VanDuijn, M. M., Inman, J. L., Fletcher, D. A. & Bissell, M. J. Tissue geometry determines sites of mammary branching morphogenesis in organotypic cultures. *Science* (80-.). **314**, 298–300 (2006).
129. Trappmann, B. *et al.* Matrix degradability controls multicellularity of 3D cell migration. *Nat. Commun.* **8**, 371 (2017).
130. Legant, W. R. *et al.* Microfabricated tissue gauges to measure and manipulate forces from 3D microtissues. *Proc. Natl. Acad. Sci. USA* **106**, 10097–10102 (2009).
131. Chen, Z. *et al.* Lung Microtissue Array to Screen the Fibrogenic Potential of Carbon Nanotubes. *Sci. Rep.* **6**, 31304 (2016).
132. Bissell, M. J., Hall, H. G. & Parry, G. How does the extracellular matrix direct gene expression? *J. Theor. Biol.* **99**, 31–68 (1982).
133. Vedula, S. R. K. *et al.* Epithelial bridges maintain tissue integrity during collective cell migration. *Nat. Mater.* **13**, 87–96 (2014).
134. Roca-Cusachs, P., Conte, V. & Trepap, X. Quantifying forces in cell biology. *Nat. Cell Biol.* **19**, 742–751 (2017).
135. A-Hassan, E. *et al.* Relative Microelastic Mapping of Living Cells by Atomic Force Microscopy. *Biophys. J.* **74**, 1564–1578 (1998).
136. Fernandez-Sanchez, M. E. *et al.* Mechanical induction of the tumorigenic beta-catenin pathway by tumour growth pressure. *Nature* **523**, 92–95 (2015).
137. Yao, M. *et al.* Force-dependent conformational switch of α -catenin controls vinculin binding. *Nat. Commun.* **5**, 4525 (2014).
138. Bambardekar, K., Clement, R., Blanc, O., Chardes, C. & Lenne, P. F. Direct laser manipulation reveals the mechanics of cell contacts in vivo. *Proc. Natl. Acad. Sci. USA* **112**, 1416–1421 (2015).
139. Evans, E. & Yeung, A. Apparent viscosity and cortical tension of blood granulocytes determined by micropipet aspiration. *Biophys. J.* **56**, 151–160 (1989).
140. Moeendarbary, E. *et al.* The cytoplasm of living cells behaves as a poroelastic material. *Nat. Mater.* **12**, 253 (2013).
141. Li, Q. S., Lee, G. Y. H., Ong, C. N. & Lim, C. T. AFM indentation study of breast cancer cells. *Biochem. Biophys. Res. Commun.* **374**, 609–613 (2008).
142. Roan, E., Wilhelm, K. R. & Waters, C. M. Kymographic Imaging of the Elastic Modulus of Epithelial Cells during the Onset of Migration. *Biophys. J.* **109**, 2051–2057 (2015).
143. Koser, D. E. *et al.* Mechanosensing is critical for axon growth in the developing brain. *Nat. Neurosci.* **19**, 1592 (2016).
144. Sugimura, K., Lenne, P.-F. & Graner, F. Measuring forces and stresses *in situ* in living tissues. *Development* **143**, 186–196 (2016).
145. Weber, G. F., Bjerke, M. A. & DeSimone, D. W. A Mechanoresponsive Cadherin-Keratin Complex Directs Polarized Protrusive Behavior and Collective Cell Migration. *Dev. Cell* **22**, 104–115 (2012).

146. Marjoram, R. J., Guilluy, C. & Burridge, K. Using magnets and magnetic beads to dissect signaling pathways activated by mechanical tension applied to cells. *Methods* **94**, 19–26 (2016).
147. Huh, D. *et al.* Reconstituting Organ-Level Lung Functions on a Chip. *Science* (80-.). **328**, 1662–1668 (2010).
148. Kim, H. J., Huh, D., Hamilton, G. & Ingber, D. E. Human gut-on-a-chip inhabited by microbial flora that experiences intestinal peristalsis-like motions and flow. *Lab Chip* **12**, 2165–2174 (2012).
149. Hart, K. C. *et al.* E-cadherin and LGN align epithelial cell divisions with tissue tension independently of cell shape. *Proc. Natl. Acad. Sci. USA* **114**, E5845–E5853 (2017).
150. Gudipaty, S. A. *et al.* Mechanical stretch triggers rapid epithelial cell division through Piezo1. *Nature* **543**, 118 (2017).
151. Cartagena-Rivera, A. X., Van Itallie, C. M., Anderson, J. M. & Chadwick, R. S. Apical surface supracellular mechanical properties in polarized epithelium using noninvasive acoustic force spectroscopy. *Nat. Commun.* **8**, 1030 (2017).
152. Jurchenko, C. & Salaita, K. S. Lighting Up the Force: Investigating Mechanisms of Mechanotransduction Using Fluorescent Tension Probes. *Mol. Cell. Biol.* **35**, 2570–2582 (2015).
153. Cai, D. *et al.* Mechanical Feedback through E-Cadherin Promotes Direction Sensing during Collective Cell Migration. *Cell* **157**, 1146–1159 (2014).
154. Grashoff, C. *et al.* Measuring mechanical tension across vinculin reveals regulation of focal adhesion dynamics. *Nature* **466**, 263 (2010).
155. Eder, D., Basler, K. & Aegerter, C. M. Challenging FRET-based E-Cadherin force measurements in *Drosophila*. *Sci. Rep.* **7**, 13692 (2017).
156. Kumar, S. *et al.* Viscoelastic Retraction of Single Living Stress Fibers and Its Impact on Cell Shape, Cytoskeletal Organization, and Extracellular Matrix Mechanics. *Biophys. J.* **90**, 3762–3773 (2006).
157. Bonnet, I. *et al.* Mechanical state, material properties and continuous description of an epithelial tissue. *J. R. Soc. Interface* **9**, 2614 LP-2623 (2012).
158. Farhadifar, R., Röper, J.-C., Aigouy, B., Eaton, S. & Jülicher, F. The Influence of Cell Mechanics, Cell-Cell Interactions, and Proliferation on Epithelial Packing. *Curr. Biol.* **17**, 2095–2104 (2007).
159. Vig, D. K., Hamby, A. E. & Wolgemuth, C. W. On the Quantification of Cellular Velocity Fields. *Biophys. J.* **110**, 1469–1475 (2016).
160. du Roure, O. *et al.* Force mapping in epithelial cell migration. *Proc. Natl. Acad. Sci. USA* **102**, 2390–2395 (2005).
161. Dembo, M. & Wang, Y.-L. Stresses at the Cell-to-Substrate Interface during Locomotion of Fibroblasts. *Biophys. J.* **76**, 2307–2316 (1999).
162. Campàs, O. *et al.* Quantifying cell-generated mechanical forces within living embryonic tissues. *Nat. Methods* **11**, 183 (2014).
163. Bergert, M. *et al.* Confocal reference free traction force microscopy. *Nat. Commun.* **7**, 12814 (2016).
164. Malinverno, C. *et al.* Endocytic reawakening of motility in jammed epithelia. *Nat. Mater.* **16**, 587 (2017).

165. Hall, M. S. *et al.* Toward single cell traction microscopy within 3D collagen matrices. *Exp. Cell Res.* **319**, 2396–2408 (2013).
166. Gjorevski, N., S. Piotrowski, A., Varner, V. D. & Nelson, C. M. Dynamic tensile forces drive collective cell migration through three-dimensional extracellular matrices. *Sci. Rep.* **5**, 11458 (2015).
167. Tambe, D. T. *et al.* Monolayer Stress Microscopy: Limitations, Artifacts, and Accuracy of Recovered Intercellular Stresses. *PLoS One* **8**, e55172 (2013).
168. Nier, V. *et al.* Inference of Internal Stress in a Cell Monolayer. *Biophys. J.* **110**, 1625–1635 (2016).
169. Ishihara, S. & Sugimura, K. Bayesian inference of force dynamics during morphogenesis. *J. Theor. Biol.* **313**, 201–211 (2012).
170. Ishihara, S. *et al.* Comparative study of non-invasive force and stress inference methods in tissue. *Eur Phys J E Soft Matter* **36**, (2013).
171. Dolega, M. E. *et al.* Cell-like pressure sensors reveal increase of mechanical stress towards the core of multicellular spheroids under compression. *Nat. Commun.* **8**, 14056 (2017).
172. Mohagheghian, E. *et al.* Quantifying compressive forces between living cell layers and within tissues using elastic round microgels. *Nat. Commun.* **9**, 1878 (2018).
173. Trepat, X. *et al.* Universal physical responses to stretch in the living cell. *Nature* **447**, 592 (2007).
174. Zhou, E. H. *et al.* Universal behavior of the osmotically compressed cell and its analogy to the colloidal glass transition. *Proc. Natl. Acad. Sci. USA* **106**, 10632–10637 (2009).
175. Xu, J., Tseng, Y. & Wirtz, D. Strain Hardening of actin filament networks regulation by the dynamic cross-linking protein α -actinin. *J. Biol. Chem.* **275**, 35886–35892 (2000).
176. Pruitt, B. L., Dunn, A. R., Weis, W. I. & Nelson, W. J. Mechano-transduction: from molecules to tissues. *PLoS Biol.* **12**, e1001996 (2014).
177. David, R. *et al.* Tissue cohesion and the mechanics of cell rearrangement. *Development* **141**, 3672–3682 (2014).
178. Seddiki, R. *et al.* Force-dependent binding of vinculin to α -catenin regulates cell-cell contacts stability and collective cell behavior. *Mol. Biol. Cell* mbc. E17-04-0231 (2017).
179. Ranft, J. *et al.* Fluidization of tissues by cell division and apoptosis. *Proc. Natl. Acad. Sci. USA* **107**, 20863–20868 (2010).
180. Harris, A. R. *et al.* Characterizing the mechanics of cultured cell monolayers. *Proc. Natl. Acad. Sci. USA* **109**, 16449–16454 (2012).
181. Thoumine, O. & Ott, A. Time scale dependent viscoelastic and contractile regimes in fibroblasts probed by microplate manipulation. *J. Cell Sci.* **110**, 2109–2116 (1997).
182. Trepat, X. *et al.* Physical forces during collective cell migration. *Nat. Phys.* **5**, 426–430 (2009).
183. Gardel, M. L., Kasza, K. E., Brangwynne, C. P., Liu, J. & Weitz, D. A. Mechanical response of cytoskeletal networks. *Methods Cell Biol.* **89**, 487–519 (2008).
184. Dalhaimer, P., Discher, D. E. & Lubensky, T. C. Crosslinked actin networks show liquid crystal elastomer behaviour, including soft-mode elasticity. *Nat. Phys.* **3**, 354–360 (2007).

185. Stricker, J., Falzone, T. & Gardel, M. L. Mechanics of the F-actin cytoskeleton. *J. Biomech.* **43**, 9–14 (2010).
186. Gardel, M. L. *et al.* Elastic behavior of cross-linked and bundled actin networks. *Science* (80-). **304**, 1301–1305 (2004).
187. Janmey, P. A., Hvidt, S., Lamb, J. & Stossel, T. P. Resemblance of actin-binding protein/actin gels to covalently crosslinked networks. *Nature* **345**, 89 (1990).
188. MacKintosh, F. C., Käs, J. & Janmey, P. A. Elasticity of semiflexible biopolymer networks. *Phys. Rev. Lett.* **75**, 4425 (1995).
189. Storm, C., Pastore, J. J., MacKintosh, F. C., Lubensky, T. C. & Janmey, P. A. Nonlinear elasticity in biological gels. *Nature* **435**, 191 (2005).
190. Kang, H. *et al.* Nonlinear elasticity of stiff filament networks: strain stiffening, negative normal stress, and filament alignment in fibrin gels. *J. Phys. Chem. B* **113**, 3799–3805 (2009).
191. Vader, D., Kabla, A., Weitz, D. & Mahadevan, L. Strain-induced alignment in collagen gels. *PLoS One* **4**, e5902 (2009).
192. Žagar, G., Onck, P. R. & van der Giessen, E. Two fundamental mechanisms govern the stiffening of cross-linked networks. *Biophys. J.* **108**, 1470–1479 (2015).
193. Koenderink, G. H. *et al.* An active biopolymer network controlled by molecular motors. *Proc. Natl. Acad. Sci. USA* **106**, 15192–15197 (2009).
194. Kim, T., Gardel, M. L. & Munro, E. D. Determinants of fluidlike behavior and effective viscosity in cross-linked actin networks. *Biophys. J.* **106**, 526–534 (2014).
195. Wilson, C. A. *et al.* Myosin II contributes to cell-scale actin network treadmilling through network disassembly. *Nature* **465**, 373 (2010).
196. Banerjee, D. S., Munjal, A., Lecuit, T. & Rao, M. Actomyosin pulsation and flows in an active elastomer with turnover and network remodeling. *Nat. Commun.* **8**, 1121 (2017).
197. Köhler, S., Schaller, V. & Bausch, A. R. Structure formation in active networks. *Nat. Mater.* **10**, 462 (2011).
198. Schuppler, M., Keber, F. C., Kröger, M. & Bausch, A. R. Boundaries steer the contraction of active gels. *Nat. Commun.* **7**, 13120 (2016).
199. Alvarado, J., Sheinman, M., Sharma, A., MacKintosh, F. C. & Koenderink, G. H. Molecular motors robustly drive active gels to a critically connected state. *Nat. Phys.* **9**, 591–597 (2013).
200. Weirich, K. L. *et al.* Liquid behavior of cross-linked actin bundles. *Proc. Natl. Acad. Sci. USA* **114**, 2131–2136 (2017).
201. Furukawa, R., Kundra, R. & Fechheimer, M. Formation of liquid crystals from actin filaments. *Biochemistry* **32**, 12346–12352 (1993).
202. Dupont, S. *et al.* Role of YAP/TAZ in mechanotransduction. *Nature* **474**, 179 (2011).
203. Panciera, T., Azzolin, L., Cordenonsi, M. & Piccolo, S. Mechanobiology of YAP and TAZ in physiology and disease. *Nat. Rev. Mol. Cell Biol.* **18**, 758–770 (2017).
204. Ege, N. *et al.* Quantitative Analysis Reveals that Actin and Src-Family Kinases Regulate Nuclear YAP1 and Its Export. *Cell Syst.* **6**, 692–708.e13 (2018).

205. Kim, N.-G. & Gumbiner, B. M. Adhesion to fibronectin regulates Hippo signaling via the FAK–Src–PI3K pathway. *J. Cell Biol.* **210**, 503–515 (2015).
206. Kim, N.-G., Koh, E., Chen, X. & Gumbiner, B. M. E-cadherin mediates contact inhibition of proliferation through Hippo signaling-pathway components. *Proc. Natl. Acad. Sci.* **108**, 11930–11935 (2011).
207. Aragona, M. *et al.* A Mechanical Checkpoint Controls Multicellular Growth through YAP/TAZ Regulation by Actin-Processing Factors. *Cell* **154**, 1047–1059 (2013).
208. Elosegui-Artola, A. *et al.* Force Triggers YAP Nuclear Entry by Regulating Transport across Nuclear Pores. *Cell* **171**, 1397–1410.e14 (2017).
209. van der Flier, L. G. & Clevers, H. Stem Cells, Self-Renewal, and Differentiation in the Intestinal Epithelium. *Annu. Rev. Physiol.* **71**, 241–260 (2009).
210. Steinhart, Z. & Angers, S. Wnt signaling in development and tissue homeostasis. *Development* **145**, 1477–9129 (2018).
211. Orsulic, S., Huber, O., Aberle, H., Arnold, S. & Kemler, R. E-cadherin binding prevents beta-catenin nuclear localization and beta-catenin/LEF-1-mediated transactivation. *J. Cell Sci.* **112**, 1237–1245 (1999).
212. Wang, Q., Sun, Z.-X., Allgayer, H. & Yang, H.-S. Downregulation of E-cadherin is an essential event in activating β -catenin/Tcf-dependent transcription and expression of its target genes in Pcdcd4 knockdown cells. *Oncogene* **29**, 128–138 (2009).
213. Benham-Pyle, B. W., Pruitt, B. L. & Nelson, W. J. Mechanical strain induces E-cadherin–dependent Yap1 and β -catenin activation to drive cell cycle entry. *Science (80-.)*. **348**, 1024–1027 (2015).
214. Trepatt, X. *et al.* Viscoelasticity of human alveolar epithelial cells subjected to stretch. *Am. J. Physiol. Cell. Mol. Physiol.* **287**, L1025–L1034 (2004).
215. Fernández, P., Pullarkat, P. A. & Ott, A. A master relation defines the nonlinear viscoelasticity of single fibroblasts. *Biophys. J.* **90**, 3796–3805 (2006).
216. Berret, J.-F. Local viscoelasticity of living cells measured by rotational magnetic spectroscopy. *Nat. Commun.* **7**, 10134 (2016).
217. Martens, J. C. & Radmacher, M. Softening of the actin cytoskeleton by inhibition of myosin II. *Pflügers Arch. J. Physiol.* **456**, 95–100 (2008).
218. Kollmannsberger, P., Mierke, C. T. & Fabry, B. Nonlinear viscoelasticity of adherent cells is controlled by cytoskeletal tension. *Soft Matter* **7**, 3127–3132 (2011).
219. Gullekson, C., Walker, M., Harden, J. L. & Pelling, A. E. Measuring mechanodynamics in an unsupported epithelial monolayer grown at an air–water interface. *Mol. Biol. Cell* **28**, 111–119 (2017).
220. Kanchanawong, P. *et al.* Nanoscale architecture of integrin-based cell adhesions. *Nature* **468**, 580 (2010).
221. Yao, M. *et al.* The mechanical response of talin. *Nat. Commun.* **7**, 11966 (2016).
222. Ciobanasu, C., Faivre, B. & Le Clairche, C. Actomyosin-dependent formation of the mechanosensitive talin–vinculin complex reinforces actin anchoring. *Nat. Commun.* **5**, 3095

- (2014).
223. Elosegui-Artola, A., Trepap, X. & Roca-Cusachs, P. Control of Mechanotransduction by Molecular Clutch Dynamics. *Trends Cell Biol.* **28**, 356–367 (2018).
 224. Bangasser, B. L. *et al.* Shifting the optimal stiffness for cell migration. *Nat. Commun.* **8**, 15313 (2017).
 225. Bangasser, B. L., Rosenfeld, S. S. & Odde, D. J. Determinants of Maximal Force Transmission in a Motor-Clutch Model of Cell Traction in a Compliant Microenvironment. *Biophys. J.* **105**, 581–592 (2013).
 226. De, R. & Safran, S. A. Dynamical theory of active cellular response to external stress. *Phys. Rev. E* **78**, 31923 (2008).
 227. Hoffman, L. M., Jensen, C. C., Chaturvedi, A., Yoshigi, M. & Beckerle, M. C. Stretch-induced actin remodeling requires targeting of zyxin to stress fibers and recruitment of actin regulators. *Mol. Biol. Cell* **23**, 1846–1859 (2012).
 228. Ladoux, B., Mège, R.-M. & Trepap, X. Front–Rear Polarization by Mechanical Cues: From Single Cells to Tissues. *Trends Cell Biol.* **26**, 420–433 (2016).
 229. Takeichi, M. Dynamic contacts: rearranging adherens junctions to drive epithelial remodelling. *Nat. Rev. Mol. Cell Biol.* **15**, 397 (2014).
 230. Harris, T. J. C. & Tepass, U. Adherens junctions: from molecules to morphogenesis. *Nat. Rev. Mol. Cell Biol.* **11**, 502 (2010).
 231. Manning, M. L., Foty, R. A., Steinberg, M. S. & Schoetz, E.-M. Coaction of intercellular adhesion and cortical tension specifies tissue surface tension. *Proc. Natl. Acad. Sci. USA* **107**, 12517–12522 (2010).
 232. Bi, D., Lopez, J. H., Schwarz, J. M. & Manning, M. L. Energy barriers and cell migration in densely packed tissues. *Soft Matter* **10**, 1885–1890 (2014).
 233. Yonemura, S., Wada, Y., Watanabe, T., Nagafuchi, A. & Shibata, M. α -Catenin as a tension transducer that induces adherens junction development. *Nat. Cell Biol.* **12**, 533–542 (2010).
 234. Dickinson, D. J., Nelson, W. J. & Weis, W. I. A Polarized Epithelium Organized by β - and α -Catenin Predates Cadherin and Metazoan Origins. *Science* (80-.). **331**, 1336 LP-1339 (2011).
 235. Gao, X. *et al.* in (eds. Ertl, P. & Rothbauer, M.) 55–66 (Springer New York, 2018). doi:10.1007/978-1-4939-7792-5_5
 236. Stirbat, T. V. *et al.* Multicellular aggregates: a model system for tissue rheology. *Eur. Phys. J. E* **36**, 84 (2013).
 237. Casares, L. *et al.* Hydraulic fracture during epithelial stretching. *Nat. Mater.* **14**, 343 (2015).
 238. Etournay, R. *et al.* Interplay of cell dynamics and epithelial tension during morphogenesis of the *Drosophila* pupal wing. *Elife* **4**, (2015).
 239. Kong, D., Wolf, F. & Großhans, J. Forces directing germ-band extension in *Drosophila* embryos. *Mech. Dev.* **144**, 11–22 (2017).
 240. Wyatt, T. P. J. *et al.* Emergence of homeostatic epithelial packing and stress dissipation through divisions oriented along the long cell axis. *Proc. Natl. Acad. Sci. USA* **112**, 5726–5731 (2015).

241. Duclos, G., Erenkämper, C., Joanny, J.-F. & Silberzan, P. Topological defects in confined populations of spindle-shaped cells. *Nat. Phys.* **13**, 58–62 (2017).
242. Kawaguchi, K., Kageyama, R. & Sano, M. Topological defects control collective dynamics in neural progenitor cell cultures. *Nature* **545**, 327 (2017).
243. Prost, J. *The physics of liquid crystals*. **83**, (Oxford university press, 1995).
244. Yamaguchi, N., Mizutani, T., Kawabata, K. & Haga, H. Leader cells regulate collective cell migration via Rac activation in the downstream signaling of integrin β 1 and PI3K. *Sci. Rep.* **5**, 7656 (2015).
245. Reffay, M. *et al.* Interplay of RhoA and mechanical forces in collective cell migration driven by leader cells. *Nat. Cell Biol.* **16**, 217–223 (2014).
246. Bahri, S. *et al.* The leading edge during dorsal closure as a model for epithelial plasticity: Pak is required for recruitment of the Scribble complex and septate junction formation. *Development* **137**, 2023–2032 (2010).
247. Hayer, A. *et al.* Engulfed cadherin fingers are polarized junctional structures between collectively migrating endothelial cells. *Nat. Cell Biol.* **18**, 1311–1323 (2016).
248. Rausch, S. *et al.* Polarizing cytoskeletal tension to induce leader cell formation during collective cell migration. *Biointerphases* **8**, 32 (2013).
249. Tlili, S. *et al.* Collective cell migration without proliferation: density determines cell velocity and wave velocity. *bioRxiv* 232462 (2017).
250. Vincent, R. *et al.* Active Tensile Modulus of an Epithelial Monolayer. *Phys. Rev. Lett.* **115**, 248103 (2015).
251. Blanch-Mercader, C. & Casademunt, J. Hydrodynamic instabilities, waves and turbulence in spreading epithelia. *Soft Matter* **13**, 6913–6928 (2017).
252. Kocgozlu, L. *et al.* Epithelial Cell Packing Induces Distinct Modes of Cell Extrusions. *Curr. Biol.* **26**, 2942–2950 (2016).
253. Deforet, M., Hakim, V., Yevick, H. G., Duclos, G. & Silberzan, P. Emergence of collective modes and tri-dimensional structures from epithelial confinement. *Nat. Commun.* **5**, 3747 (2014).
254. Bi, D., Yang, X., Marchetti, M. C. & Manning, M. L. Motility-driven glass and jamming transitions in biological tissues. *Phys. Rev. X* **6**, 21011 (2016).
255. Angelini, T. E. *et al.* Glass-like dynamics of collective cell migration. *Proc. Natl. Acad. Sci. USA* **108**, 4714–4719 (2011).
256. Atia, L. *et al.* Geometric constraints during epithelial jamming. *Nat. Phys.* **14**, 613–620 (2018).
257. Wilk, G., Iwasa, M., Fuller, P. E., Kandere-Grzybowska, K. & Grzybowski, B. A. Universal area distributions in the monolayers of confluent mammalian cells. *Phys. Rev. Lett.* **112**, 138104 (2014).
258. Rossen, N. S., Tarp, J. M., Mathiesen, J., Jensen, M. H. & Oddershede, L. B. Long-range ordered vorticity patterns in living tissue induced by cell division. *Nat. Commun.* **5**, 5720 (2014).
259. Doostmohammadi, A. *et al.* Cell division: a source of active stress in cellular monolayers. *Soft Matter* **11**, 7328–7336 (2015).
260. Miroshnikova, Y. A. *et al.* Adhesion forces and cortical tension couple cell proliferation and

- differentiation to drive epidermal stratification. *Nat. Cell Biol.* **20**, 69–80 (2018).
261. de la Loza, M. C. D. *et al.* Laminin Levels Regulate Tissue Migration and Anterior-Posterior Polarity during Egg Morphogenesis in *Drosophila*. *Cell Rep.* **20**, 211–223 (2017).
 262. Gopal, S. *et al.* Fibronectin-guided migration of carcinoma collectives. *Nat. Commun.* **8**, 14105 (2017).
 263. Carey, S. P., Martin, K. E. & Reinhart-King, C. A. Three-dimensional collagen matrix induces a mechanosensitive invasive epithelial phenotype. *Sci. Rep.* **7**, 42088 (2017).
 264. Thuenauer, R., Rodriguez-Boulan, E. & Römer, W. Microfluidic approaches for epithelial cell layer culture and characterisation. *Analyst* **139**, 3206–3218 (2014).
 265. Beenakker, J.-W. M., Ashcroft, B. A., Lindeman, J. H. N. & Oosterkamp, T. H. Mechanical Properties of the Extracellular Matrix of the Aorta Studied by Enzymatic Treatments. *Biophys. J.* **102**, 1731–1737 (2012).
 266. Engler, A. J., Sen, S., Sweeney, H. L. & Discher, D. E. Matrix Elasticity Directs Stem Cell Lineage Specification. *Cell* **126**, 677–689 (2006).
 267. Swift, J. *et al.* Nuclear Lamin-A Scales with Tissue Stiffness and Enhances Matrix-Directed Differentiation. *Science (80-.)*. **341**, 1240104 (2013).
 268. Van De Water, L., Varney, S. & Tomasek, J. J. Mechanoregulation of the Myofibroblast in Wound Contraction, Scarring, and Fibrosis: Opportunities for New Therapeutic Intervention. *Adv. Wound Care* **2**, 122–141 (2013).
 269. Harland, B., Walcott, S. & Sun, S. X. Adhesion Dynamics and Durotaxis in Migrating Cells. *Biophys. J.* **100**, 303a (2011).
 270. Novikova, E. A., Raab, M., Discher, D. E. & Storm, C. Persistence-Driven Durotaxis: Generic, Directed Motility in Rigidity Gradients. *Phys. Rev. Lett.* **118**, 78103 (2017).
 271. Yu, G., Feng, J., Man, H. & Levine, H. Phenomenological modeling of durotaxis. *Phys. Rev. E* **96**, 10402 (2017).
 272. Ng, M. R., Besser, A., Danuser, G. & Brugge, J. S. Substrate stiffness regulates cadherin-dependent collective migration through myosin-II contractility. *J. Cell Biol.* **199**, 545 LP-563 (2012).
 273. Martinez, J. S., Schlenoff, J. B. & Keller, T. C. S. Collective epithelial cell sheet adhesion and migration on polyelectrolyte multilayers with uniform and gradients of compliance. *Exp. Cell Res.* **346**, 17–29 (2016).
 274. Escribano, J. *et al.* A hybrid computational model for collective cell durotaxis. *Biomech. Model. Mechanobiol.* (2018). doi:10.1007/s10237-018-1010-2
 275. Nasrollahi, S. *et al.* Past matrix stiffness primes epithelial cells and regulates their future collective migration through a mechanical memory. *Biomaterials* **146**, 146–155 (2017).
 276. Yang, C., Tibbitt, M. W., Basta, L. & Anseth, K. S. Mechanical memory and dosing influence stem cell fate. *Nat. Mater.* **13**, 645 (2014).
 277. Matsuzaki, S., Darcha, C., Pouly, J.-L. & Canis, M. Effects of matrix stiffness on epithelial to mesenchymal transition-like processes of endometrial epithelial cells: Implications for the pathogenesis of endometriosis. *Sci. Rep.* **7**, 44616 (2017).

278. Wei, S. C. *et al.* Matrix stiffness drives epithelial–mesenchymal transition and tumour metastasis through a TWIST1–G3BP2 mechanotransduction pathway. *Nat. Cell Biol.* **17**, 678–688 (2015).
279. Alexander, N. R. *et al.* N-cadherin Gene Expression in Prostate Carcinoma Is Modulated by Integrin-Dependent Nuclear Translocation of Twist1. *Cancer Res.* **66**, 3365 LP-3369 (2006).
280. Paszek, M. J. *et al.* Tensional homeostasis and the malignant phenotype. *Cancer Cell* **8**, 241–254 (2005).
281. Swaminathan, V. *et al.* Mechanical Stiffness Grades Metastatic Potential in Patient Tumor Cells and in Cancer Cell Lines. *Cancer Res.* **71**, 5075 LP-5080 (2011).
282. Style, R. W. *et al.* Patterning droplets with durotaxis. *Proc. Natl. Acad. Sci. USA* **110**, 12541–12544 (2013).
283. Siedlik, M. J., Manivannan, S., Kevrekidis, I. G. & Nelson, C. M. Cell Division Induces and Switches Coherent Angular Motion within Bounded Cellular Collectives. *Biophys. J.* **112**, 2419–2427 (2017).
284. Tanner, K., Mori, H., Mroue, R., Bruni-Cardoso, A. & Bissell, M. J. Coherent angular motion in the establishment of multicellular architecture of glandular tissues. *Proc. Natl. Acad. Sci. USA* **109**, 1973–1978 (2012).
285. Boghaert, E. *et al.* Host epithelial geometry regulates breast cancer cell invasiveness. *Proc. Natl. Acad. Sci. USA* **109**, 19632–19637 (2012).
286. Labernadie, A. *et al.* A mechanically active heterotypic E-cadherin/N-cadherin adhesion enables fibroblasts to drive cancer cell invasion. *Nat. Cell Biol.* **19**, 224–237 (2017).
287. Haga, H., Irahara, C., Kobayashi, R., Nakagaki, T. & Kawabata, K. Collective Movement of Epithelial Cells on a Collagen Gel Substrate. *Biophys. J.* **88**, 2250–2256 (2005).
288. Londono, C. *et al.* Nonautonomous contact guidance signaling during collective cell migration. *Proc. Natl. Acad. Sci. USA* **111**, 1807–1812 (2014).
289. Nam, K.-H. *et al.* Multiscale Cues Drive Collective Cell Migration. *Sci. Rep.* **6**, 29749 (2016).
290. Uttayarat, P., Toworfe, G. K., Dietrich, F., Lelkes, P. I. & Composto, R. J. Topographic guidance of endothelial cells on silicone surfaces with micro- to nanogrooves: Orientation of actin filaments and focal adhesions. *J. Biomed. Mater. Res. Part A* **75A**, 668–680 (2005).
291. Attieh, Y. *et al.* Cancer-associated fibroblasts lead tumor invasion through integrin- β 3–dependent fibronectin assembly. *J Cell Biol* jcb. 201702033 (2017).
292. Weigel, B., Bakker, G.-J. & Friedl, P. Intravital third harmonic generation microscopy of collective melanoma cell invasion. *IntraVital* **1**, 32–43 (2012).
293. Haeger, A., Krause, M., Wolf, K. & Friedl, P. Cell jamming: Collective invasion of mesenchymal tumor cells imposed by tissue confinement. *Biochim. Biophys. Acta - Gen. Subj.* **1840**, 2386–2395 (2014).
294. Dukes, J. D., Whitley, P. & Chalmers, A. D. The MDCK variety pack: choosing the right strain. *BMC Cell Biol.* **12**, 43 (2011).
295. Rodríguez-Fraticelli, A. E., Auzan, M., Alonso, M. A., Bornens, M. & Martín-Belmonte, F. Cell confinement controls centrosome positioning and lumen initiation during epithelial morphogenesis. *J. Cell Biol.* **198**, 1011–1023 (2012).

296. Imai, M., Furusawa, K., Mizutani, T., Kawabata, K. & Haga, H. Three-dimensional morphogenesis of MDCK cells induced by cellular contractile forces on a viscous substrate. *Sci. Rep.* **5**, 14208 (2015).
297. Martín-Belmonte, F. *et al.* Cell-Polarity Dynamics Controls the Mechanism of Lumen Formation in Epithelial Morphogenesis. *Curr. Biol.* **18**, 507–513 (2008).
298. Jaffe, A. B., Kaji, N., Durgan, J. & Hall, A. Cdc42 controls spindle orientation to position the apical surface during epithelial morphogenesis. *J. Cell Biol.* **183**, 625–633 (2008).
299. Dasgupta, S., Gupta, K., Zhang, Y., Viasnoff, V. & Prost, J. Physics of lumen growth. *Proc. Natl. Acad. Sci.* DOI: 10.1073/pnas.1722154115 (2018).
300. Sugahara, K., Caldwell, J. H. & Mason, R. J. Electrical currents flow out of domes formed by cultured epithelial cells. *J. Cell Biol.* **99**, 1541–1544 (1984).
301. Hannezo, E., Prost, J. & Joanny, J.-F. Theory of epithelial sheet morphology in three dimensions. *Proc. Natl. Acad. Sci.* **111**, 27–32 (2014).
302. Hannezo, E., Prost, J. & Joanny, J.-F. Instabilities of Monolayered Epithelia: Shape and Structure of Villi and Crypts. *Phys. Rev. Lett.* **107**, 78104 (2011).
303. Levina, E. M., Domnina, L. V, Rovensky, Y. A. & Vasiliev, J. M. Cylindrical substratum induces different patterns of actin microfilament bundles in nontransformed and in ras-transformed epitheliocytes. *Exp. Cell Res.* **229**, 159–165 (1996).
304. Svitkina, T. M., Rovensky, Y. A., Bershinsky, A. D. & Vasiliev, J. M. Transverse pattern of microfilament bundles induced in epitheliocytes by cylindrical substrata. *J. Cell Sci.* **108**, 735–745 (1995).
305. Biton, Y. Y. & Safran, S. A. The cellular response to curvature-induced stress. *Phys. Biol.* **6**, 46010 (2009).
306. Sun, B., Xie, K., Chen, T.-H. & Lam, R. H. W. Preferred cell alignment along concave microgrooves. *RSC Adv.* **7**, 6788–6794 (2017).
307. Park, J. Y., Lee, D. H., Lee, E. J. & Lee, S.-H. Study of cellular behaviors on concave and convex microstructures fabricated from elastic PDMS membranes. *Lab Chip* **9**, 2043–2049 (2009).
308. Werner, M. *et al.* Surface curvature differentially regulates stem cell migration and differentiation via altered attachment morphology and nuclear deformation. *Adv. Sci.* **4**, 1600347 (2017).
309. Qian, J., Wang, J., Lin, Y. & Gao, H. Lifetime and Strength of Periodic Bond Clusters between Elastic Media under Inclined Loading. *Biophys. J.* **97**, 2438–2445 (2009).
310. Gao, H., Qian, J. & Chen, B. Probing mechanical principles of focal contacts in cell–matrix adhesion with a coupled stochastic–elastic modelling framework. *J. R. Soc. Interface* **8**, 1217 LP-1232 (2011).
311. Bade, N. D., Kamien, R. D., Assoian, R. K. & Stebe, K. J. Curvature and Rho activation differentially control the alignment of cells and stress fibers. *Sci. Adv.* **3**, e1700150 (2017).
312. Napoli, G. & Vergori, L. Extrinsic curvature effects on nematic shells. *Phys. Rev. Lett.* **108**, 207803 (2012).
313. Solon, J., Kaya-Çopur, A., Colombelli, J. & Brunner, D. Pulsed Forces Timed by a Ratchet-like Mechanism Drive Directed Tissue Movement during Dorsal Closure. *Cell* **137**, 1331–1342 (2009).

314. Honda, H. Description of cellular patterns by Dirichlet domains: The two-dimensional case. *J. Theor. Biol.* **72**, 523–543 (1978).
315. Graner, F. & Glazier, J. A. Simulation of biological cell sorting using a two-dimensional extended Potts model. *Phys. Rev. Lett.* **69**, 2013–2016 (1992).
316. Kabla, A. J. Collective cell migration: leadership, invasion and segregation. *J. R. Soc. Interface* **9**, 3268 LP-3278 (2012).
317. Gomez, L. C. and H. L. and I.-M. S. and A. S. Y. and V. L. and G. A. Role of contact inhibition of locomotion and junctional mechanics in epithelial collective responses to injury. *Phys. Biol.* **15**, 24001 (2018).
318. Kopf, M. H. & Pismen, L. M. A continuum model of epithelial spreading. *Soft Matter* **9**, 3727–3734 (2013).
319. Van Liedekerke, P., Palm, M. M., Jagiella, N. & Drasdo, D. Simulating tissue mechanics with agent-based models: concepts, perspectives and some novel results. *Comput. Part. Mech.* **2**, 401–444 (2015).
320. Hakim, V. & Silberzan, P. Collective cell migration: a physics perspective. *Reports Prog. Phys.* **80**, 76601 (2017).
321. Camley, B. A. & Rappel, W.-J. Physical models of collective cell motility: from cell to tissue. *J. Phys. D. Appl. Phys.* **50**, 113002 (2017).
322. Voss-Böhme, A. Multi-Scale Modeling in Morphogenesis: A Critical Analysis of the Cellular Potts Model. *PLoS One* **7**, e42852 (2012).
323. Fletcher, A. G., Osterfield, M., Baker, R. E. & Shvartsman, S. Y. Vertex Models of Epithelial Morphogenesis. *Biophys. J.* **106**, 2291–2304 (2014).
324. Giavazzi, F. *et al.* Flocking transitions in confluent tissues. *Soft Matter* **14**, 3471–3477 (2018).
325. Szabó, C. A. *et al.* Collective cell motion in endothelial monolayers. *Phys. Biol.* **7**, 46007 (2010).
326. Toner, J., Tu, Y. & Ramaswamy, S. Hydrodynamics and phases of flocks. *Ann. Phys. (N. Y.)* **318**, 170–244 (2005).
327. Marchetti, M. C. *et al.* Hydrodynamics of soft active matter. *Rev. Mod. Phys.* **85**, 1143 (2013).
328. Thampi, S. P., Golestanian, R. & Yeomans, J. M. Instabilities and topological defects in active nematics. *EPL (Europhysics Lett.)* **105**, 18001 (2014).
329. Thampi, S. P., Golestanian, R. & Yeomans, J. M. Vorticity, defects and correlations in active turbulence. *Phil. Trans. R. Soc. A* **372**, 20130366 (2014).